

620.51  
P975c  
1961  
No. 11

# REPORT NO. 4

## HYDRAULICS OF SINGLE SPAN ARCH BRIDGE CONSTRICTIONS

MAY 1961

661780

NO. 11

Joint  
Highway  
Research  
Project

PURDUE UNIVERSITY  
LAFAYETTE INDIANA

by

P. F. BIERY  
J. W. DELLEUR



Report No. 4

Hydraulics of Single Span Arch Bridge Constrictions

by

P. F. Biery

Research Engineer, Johns Manville, Inc., Manville, N.J.  
formerly Research Assistant, Purdue University

and

J. W. Delleur

Associate Professor of Hydraulic Engineering

State Highway Department of Indiana  
in Cooperation with  
U.S. Department of Commerce  
Bureau of Public Roads

Joint Highway Research Project  
Project No. G-36-62B  
File No. 9-8-2

Purdue University  
School of Civil Engineering  
Hydraulic Laboratory

May, 1961



# HYDRAULICS OF SINGLE SPAN ARCH BRIDGE CONSTRICTION<sup>1</sup>

by P. F. Biery<sup>2</sup>, AM-ASCE and J. W. Delleur<sup>3</sup>, M-ASCE

## Synopsis

The results of model testing of semicircular arch bridge constrictions are presented. All tests were run for the condition of no skew, no eccentricity and no entrance rounding. A generalized backwater equation is presented, by means of which one can evaluate the backwater superlevation in terms of the bridge span, the stream width and the Froude number of the approaching flow. The equation holds for geometries other than semicircular constrictions. Design procedures for indirect discharge measurement, for determination of backwater superlevation, and for determination of required waterway area are given. A model-prototype comparison is discussed.

- 
- 1 - Presented at the national ASCE convention, Hydraulic Division, Hydraulic Structures Session, October 14, 1960
  - 2 - Research Engineer, Johns Manville, Inc., Manville, New Jersey, formerly Research Assistant, School of Civil Engineering, Purdue University
  - 3 - Associate Professor of Hydraulic Engineering, School of Civil Engineering, Purdue University, Lafayette, Indiana



## INTRODUCTION

In recent years, the problem of protecting the flood plains from flood damage has become increasingly important. In order to eliminate or minimize any additional flood effects, the highway engineer must be able to predict the influence of a new highway bridge upon river stages during high flood flows. It is generally recognized that the introduction of a bridge crossing interferes with the natural flow of the stream and results in a rise in stage upstream and an increase in velocity through the bridge. It is the highway engineer's responsibility to provide the minimum span length for structural and economic reasons, and yet to allow a large enough water area to keep the rise in backwater within tolerable limits. Without the necessary information to make an intelligent estimate of the maximum backwater, overdesign or underdesign results in making either the cost of the bridge prohibitive or the risk of flood damage excessive.

In the past, studies by the U. S. Geological Survey and the Bureau of Public Roads pertaining to the backwater effects caused by bridge constrictions have considered shapes of openings such as those produced by straight deck bridges. However, very little has been done in the way of making a systematic study of the hydraulics of river flow under the various shapes of arch bridges. The arch is unique in that the surface width of the water surface within the barrel of the arch decreases with a corresponding increase in stage.

A project was initiated in the Hydraulics Laboratory at Purdue University to study the hydraulics of stream flow under arch bridges. It is sponsored by the Indiana State Highway Department in cooperation with

Digitized by the Internet Archive  
in 2011 with funding from  
LYRASIS members and Sloan Foundation; Indiana Department of Transportation



the U. S. Bureau of Public Roads. The purpose of this research is to study the hydraulics of arch bridge constrictions and to provide a method for computing the backwater upstream of the bridge.

The earliest systematic laboratory investigation of flow through contractions in open channels was performed by E. W. Lane.<sup>1\*</sup> He related the discharge and the water surface elevation through the contraction by means of empirical discharge coefficients, and indicated that there may exist some relationship between these coefficients and the ratio of the maximum backwater depth produced by the contraction to the normal depth of flow without the contraction. This ratio is referred to as the backwater ratio.

In 1955, Kindsvater and Carter<sup>2</sup> presented a practical solution to the discharge equation by an extensive experimental investigation. By applying correction terms for various geometric conditions to a standard discharge coefficient, the method can be applied to a wide variety of boundary conditions. A detailed description of the internal and external flow characteristics was given.

In the same year, H. J. Tracy and R. W. Carter<sup>3</sup> presented a companion paper to the one by Kindsvater and Carter. In it they gave a method of computing the nominal backwater due to open channel constrictions. The practical solution was based upon empirical discharge coefficients and a laboratory investigation of the influence of channel roughness, channel shape, and constriction geometry. Their study was limited to single span, deck type constrictions and to steady tranquil flow. C. F. Izzard,<sup>4</sup> in his discussion of this paper, pointed out that the backwater ratio expressed as  $y_1/y_n$  (see Figure 1) is a function of the normal depth

\* Superscripts refer to references in the bibliography.



Froude number at the constricted section. Also, he questioned the use of the backwater ratio in terms of  $h_1^2/\Delta h$  when the head loss between the section of maximum backwater and the vena contracta is large compared to the approach velocity head.

In 1953, some of the combined efforts of Kindsvater, Carter, and Tracy were organized into a U. S. Geological Survey Circular<sup>5</sup>. It presented a method for determining peak discharge at abrupt contractions. The discharge estimate was to be made from a survey of high water marks and channel characteristics. Although the method applies well to deck type bridges, there is no direct application for using the method when an arch bridge is used to make an indirect measurement.

In October 1957, the Colorado State University in cooperation with the U. S. Bureau of Public Roads published a bulletin by H. K. Liu<sup>6</sup>, J. N. Bradley and E. J. Plate entitled "Backwater Effects of Piers and Abutments". A rigorous and extensive investigation of the backwater effects of piers and abutments has been given. The paper includes a complete analysis of the energy losses through the constriction. An approximate simple method of analysis is provided for the highway engineer to use. The general principle of the method is the conservation of energy. A number of graphs based upon laboratory data were developed for determining the maximum backwater and the differential level of water surface elevations across the embankment. Much of the work done at Colorado has been used as a comparison to the present research.

Based upon the model tests conducted at Colorado State University, J. N. Bradley<sup>7</sup> compiled a report entitled "Hydraulics of Bridge Waterways". The publication was completed in August 1960 and is the first in a series of reports on the hydraulic design of highway drainage structures. This



particular report, within limitations, is intended to provide a means of computing the effect of a given bridge upon the flow in a stream.

H. R. Vallentine<sup>8</sup> reports on tests performed to study the characteristics of flow in a rectangular channel with symmetrically placed sharp edged constriction plates placed normal to the flow. The flow is related to the upstream depth by means of a weir type discharge equation. The experimental coefficients were found to depend upon the geometry of the constriction and the Froude number of the unconstricted flow. The conditions which produce an increase in the upstream depth were investigated and the extent of the increase evaluated.

Some recent work done at Lehigh University<sup>9</sup> tells about the effects of placing spur dikes on the upstream side of a bridge contraction. These dikes are designed to increase the hydraulic efficiency of the bridge crossing by lowering the backwater curve and reducing the scour underneath the bridge. This particular report presents a good qualitative description of the flow patterns through the bridge embankments.

A preliminary investigation including some model testing of semi-circular arch constrictions was done at Purdue University by Owen, Sooky, Hussin and Delleur<sup>10</sup> in 1958 and 1959. The backwater superlevation was related to the Froude number of the approaching flow and to the ratio of the arch span to the stream width. The present paper is an outgrowth of this preliminary study.



## THEORETICAL ANALYSIS

### Dimensional Considerations

Figure 1 shows a definition sketch of the effects of a channel constriction on the water surface profile. Section view B illustrates the type of centerline profile obtained with a mild slope channel. This is the most generally occurring situation that appears in actual practice. In the figure  $y_0$  or  $y_n$  is the normal depth of the unobstructed channel,  $y_1$  is the depth at the point of maximum backwater elevation,  $y_2$  is the depth at the section of minimum jet area or the vena contracta,  $y_3$  is the minimum water depth of the regain curve, and  $y_4$  is at a point sufficiently downstream from the contraction where the flow returns to the normal depth.

A dimensional analysis was made for the purpose of guidance and interpretation of the testing program. In this manner the basic variables can be grouped into dimensionless quantities and their relationships investigated. In the problem at hand, it is desired to determine the maximum water depth upstream of the constriction. It is assumed that the variables which govern the backwater super-elevation may be grouped into three categories as follows: the fluid properties, the kinematic and dynamic variables, and the dimensions defining the boundary geometry. Due to the two dimensional character of the constriction, the latter is expressed in terms of flow areas rather than the usual linear dimensions.

The variables are: (see Figure 1)

a.) Fluid Properties

$\nu$ , the kinematic viscosity of the fluid

$\rho$ , density of the fluid

b.) Kinematic and Dynamic Flow Variables

$g$ , acceleration of gravity





- $y_1$ , maximum water depth upstream of the constriction.  
(section 1)
- $y_n$ , the normal depth of flow in the approach channel.  
(section 0)
- $V_n$ , the velocity of flow at normal depth
- $n$ , Manning's roughness coefficient of the approach  
channel
- $\Delta h$ , the maximum water surface drop across the constric-  
tion ( $\Delta h = y_1 - y_3$ )

c.) Properties of the Constriction Geometry

- $A_{n1}$ , the total normal depth flow area at section 1
- $A_{n2}$ , the normal depth flow area at the upstream fact of  
the constriction

Hence, from the above list of variables,

$$y_1 = f_1 (V_n, V_n, n, \Delta h, V, \rho, g, A_{n1}, A_{n2}) \quad \text{---(1)}$$

Buckingham's theorem<sup>11</sup> states that in a physical problem including  $n$  quantities in which there are  $m$  dimensions, the quantities may be arranged into  $(n - m)$  dimensionless parameters. With the mass, length and time systems of units the  $n-4$  or seven dimensionless  $\pi$  parameters are as follows,

$$y_1 / y_n = f_2 (y_{n2} / y_n^2, V / V_n y_n, n / y_n^{1/6}, A_{n1} / y_n^2, A_{n2} / y_n^2, \Delta h / y_n) \quad \text{---(2)}$$

Inverting the first two parameters

$$y_1 / y_n = f_3 (V_n^2 / y_n g, V_n y_n / \rho, n / y_n^{1/6}, A_{n1} / y_n^2, A_{n2} / y_n^2, \Delta h / y_n) \quad \text{---(3)}$$

In equation (3) the term  $V_n^2 / g y_n$  is the square of the normal depth Froude number. It is well known that gravity forces are predominant in open channel flow whereas viscous forces play a secondary role. The Reynolds number  $V_n y_n / \nu$  may be disregarded in the determination of  $y_1 / y_n$ . Furthermore, by assuming that the shape of the water surface upstream is not materially affected by the shape of the water surface downstream, the term  $\Delta h / y_n$  can



also be eliminated. By combining the ratios  $A_{n2}/y_n^2$  and  $A_{n1}/y_n^2$  into  $A_{n2}/y_n^2$  and excluding the above mentioned terms, equation (3) becomes,

$$y_1/y_n = f_4(F_n^2, y_n^{1/2}/n, A_{n2}/A_{n1}) \quad \text{--- (1)}$$

The backwater ratio is therefore expected to be a function of the normal depth Froude number, the channel roughness and the ratio  $A_{n2}/A_{n1}$ .

The channel opening ratio ( $M'$ ) is defined as that portion of the total normal depth flow which can pass through the bridge waterway without contraction.

Referring to figure 2a, for the rectangular case, the total flow in area ABDE is  $Q$  and the flow passing through the bridge opening without contraction, that is in the area BCFG, is  $q$ . Therefore the opening ratio  $M'$  is

$$M' = q/Q$$

If we assume that there is a constant uniform velocity  $V_n$  across the entire normal depth section, equation (5) becomes

$$M' = q/Q = A_{n2}V_n/A_{n1}V_n = A_{n2}/A_{n1} = by_n/By_n = b/B \quad \text{--- (6)}$$

However, for an arch bridge, as shown also in figure 2b, the surface width will be different for each and every normal depth  $y_n$ . Therefore in the same manner,

$$M' = q/Q = A_{n2}V_n/A_{n1}V_n = A_{n2}/A_{n1} \quad \text{--- (7)}$$

The ratio of the two areas is clearly not equivalent to  $b/B$ . (For simplicity,  $b/B$  is hereafter defined by the symbol  $M$ )

The portion GHEF (Figure 2b) below the depth  $y_n$  of a semicircular arch of radius  $r$  has an area

$$A_{n2} = \int_0^{y_n} 2\sqrt{r^2 - y^2} dy = 2 \left[ \frac{1}{2} \{ y_n \sqrt{r^2 - y_n^2} + r^2 \sin^{-1} y_n/r \} \right] \quad \text{--- (8)}$$

The segment of arch GHEF shown in figure 2b has a radius  $r$  and springline width  $b$ . Its center is at a distance  $d$  below the springline of the arch.



The area of the arch segment GBCF is

$$A_{n2} = \int_0^D 2\sqrt{r^2 - y^2} dy = \int_0^d 2\sqrt{r^2 - y^2} dy \quad \text{---(9)}$$

and the corresponding channel opening ratio is:

$$M^0 = A_{n2}/A_{n1} = \frac{D\sqrt{r^2 - D^2} + r^2 \sin^{-1}D/r}{By_n} = \frac{d\sqrt{r^2 - d^2} + r^2 \sin^{-1}d/r}{By_n} \quad \text{---(10)}$$

The channel opening ratio  $M^0$  can be expressed in terms of three dimensionless ratios; the ratio of span to channel width  $M = b/B$ , the ratio of depth of the arch center below the streambed to the arch radius  $\eta = d/r$  and the ratio of normal depth to arch radius  $\zeta = y_n/r$ . The channel opening ratio of equation (10) may thus be expressed as:

$$M^0 = MC_M \quad \text{---(11)}$$

where

$$M = b/B$$

and

$$C_M = 1/2 \left[ \frac{\left\{ \frac{\sqrt{1-(\eta+\zeta)^2} + (\eta+\zeta) \sin^{-1}(\eta+\zeta)}{\frac{\zeta}{\eta+\zeta} \sqrt{1-\eta^2}} \right\} - \left\{ \frac{\sqrt{1-\eta^2} + \eta \sin^{-1}\eta}{\frac{\zeta}{\eta} \sqrt{1-\eta^2}} \right\}}{2} \right] \quad \text{---(12)}$$

with

$$\eta = d/r$$

and

$$\zeta = y_n/r$$

In the form of equation (11) the value of  $M = b/B$  is adjusted for the particular arch by an amount equivalent to  $C_M$  such that  $M^0$  is the ratio of  $A_{n2}$  to  $A_{n1}$ . In the more general case, the values of  $\zeta$  and  $\eta$  can take on numbers within certain limits, before the normal depth will submerge the crown of the arch. The limits are as follows:

$$\text{For } \zeta = y_n/r \quad 0/r \leq y_n/r \leq (r-d)/r \quad \text{---(13)}$$



or

$$0 \leq \zeta \leq (1 - \eta)$$

$$\text{For } \eta = d/r \quad 0 \leq \eta \leq 1$$

When  $\eta = 0$ , the case of a semicircular arch with the center of curvature at the springline exists. When  $\eta = 1$ , the contraction reduces to two parallel abutments.

The values of  $C_M$  have been calculated for several values of  $\zeta$  and  $\eta$  and are given in the graph of Figure 3. The submergence limit represents the upper limits of both  $\zeta$  and  $\eta$ . The segment arch which is a constant radius arch with its center of curvature below the springline of the arch (i.e.  $\eta > 0$ ) can be used as an arch in its own right or as an approximation to an elliptical or a multiple radius arch. The value of  $M'$  for the elliptic and multiple radius arch could be determined directly from equation (7). However, they have not been worked out in the present research. If equation (11) were applied to vertical abutment bridge piers as idealized in Figure 2a, the value of  $C_M$  would become unity.

An approximate form of the equation for the discharge through a two dimensional semicircular arch constriction in a rectangular channel may be expressed in terms of an infinite series of powers of the  $y_1/r$ . With reference to figure 1, the Bernoulli theorem gives;

$$Q = \int V \, dA = \int_0^{y_1} C \sqrt{2g(y_1 - h)} \times 2\sqrt{r^2 - h^2} \, dh \quad \text{---(14)}$$

Expanding equation (14) into a series and integrating term by term and making use of the fact that  $2r = b$ :

$$Q = C_d \sqrt{2g} \, 17/24 \, y_1^{3/2} b \left[ 1 - 0.1294(y_1/r)^2 - 0.0177(y_1/r)^4 \right] \quad \text{---(15)}$$

This may be written as

$$Q = C_{y1}^{3/2} b \, T \quad \text{---(16)}$$

$$\text{where} \quad C = C_d \, 17/24 \sqrt{2g} \quad \text{---(17)}$$





$$\text{and } T = \left[ (1 - 0.1294(y_1/r)^2 - 0.0177(y_1/r)^4 \dots) \right] \quad \text{---(18)}$$

The discharge in a rectangular approach channel may also be expressed by

$$Q = V_n A_n = F_n \sqrt{g} B y_n^{3/2} \quad \text{---(19)}$$

where

$$F_n = V_n / \sqrt{g y_n}$$

is the Froude number of the undisturbed normal depth flow. Equating (15) and (19) and solving for the discharge coefficient

$$C_d = (12\sqrt{2} F_n / 17 M^3) (y_n / y_1)^{3/2} \quad \text{---(20)}$$

Typical values of the coefficient of discharge  $C_d$  are shown in figure 8 which shows the results of the two dimensional semicircular arch tests in the rough rectangular channel. It is interesting to note the limiting conditions of the discharge coefficient as  $M^3$  goes from zero to one. For a two dimensional ideal orifice, Streeter<sup>12</sup> shows that the application of the theory of free streamlines leads to an ideal discharge coefficient of

$$\frac{\frac{2b}{\pi} + 2b}{\pi} = \pi / (\pi + 2) = 0.611 \quad \text{---(21)}$$

The coefficient of discharge curves of figure 8 converge to 0.611 showing that this is a limiting value of  $C_d$  as  $M^3$  approaches zero.

When  $M^3$  is equal to unity,  $C_M = 1$  and  $b/B = 1$ . Therefore,  $b = B$  and there is no contraction at all. If there is no contraction, then  $y_1/y_n = 1$  and  $T = 1$ . Also  $12\sqrt{2} / 17 = 0.9981$  which is approximately unity. Therefore equation (20) becomes

$$\text{at } M^3 = 1 \quad 1 = (F_n / C_d)^{2/3}$$

Therefore as the opening ratio tends to unity, the discharge coefficient tends to the Froude number of the undisturbed flow.



### The Backwater Ratio Equation

The backwater ratio is defined as the ratio of the maximum centerline water depth to the normal depth of flow. Since  $M = M^0/C$  equation (20) may be rearranged such that the backwater ratio becomes

$$y_1/y_n = (12\sqrt{2} F_n / 17 C_d M T)^{2/3} \quad \text{---(23)}$$

It has been observed that the equations derived by several different investigators for the backwater ratio produced by various constriction geometries seem to have a basic similarity. As an example, equation (23) in the present text for  $y_1/y_n$  appears to be a function of  $(F/M^0)^{2/3}$ .

$$y_1/y_n = g_1(F_n/M^0)^{2/3} \quad \text{---(24)}$$

An equation for the backwater ratio given by Valentine<sup>5</sup> for lateral constriction plates is

$$y_1/y_n = (g F_n / C M)^{2/3} = g_2(F_n/M^0)^{2/3} \quad \text{---(25)}$$

Also Lin<sup>6</sup> presents an empirical formula for a two dimensional vertical board model

$$(h_1^*/h_n)^3 = 4.6482 F_n^2 \left( \frac{1}{M^2} - \frac{2}{3} (2.5 - M) \right) - 1 \quad \text{---(26)}$$

Considering only the leading term  $1/M^2$  of the quantity in brackets, equation (26) becomes

$$h_1^*/h_n = g_3(F_n/M^0)^{2/3} \quad \text{---(27)}$$

Therefore it appears possible that with the proper interpretation of the variables, namely  $M^0$  and  $F_n$ , the results of tests performed on different geometric shapes of bridge openings may produce the same results. For instance, a vertical abutment deck type bridge may physically appear completely different from a semicircular arch bridge. However, for hydraulic considerations, if they have the same opening ratio  $M^0$ , they may produce the same backwater ratio. The limitations of the assumption must necessarily lie in the fact that both bridges must have the same



eccentricity, skewness and entrance rounding conditions. It is believed that this concept applies equally as well to multiple span bridges. An attempt has been made to compare the two dimensional semicircular test results the segment data, and the Vertical Board (VB) data as given by Liu<sup>6</sup>. The results of this comparison in Figure 14 have substantiated the assumption of the similarity between the functions  $g_1$ ,  $g_2$  and  $g_3$ .

## EXPERIMENTAL EQUIPMENT

### Small Flume and Models

For the purpose of preliminary testing, a small variable slope flume 6" wide and 12' long was used. The channel sides and bottom were constructed of lucite and carefully aligned by means of adjusting screws. The slope of the flume was controlled by a hand operated scissor jack at the lower end of the flume. An aluminum I-beam mounted horizontally above the flume served as a track for the mechanical and electric point gages used in obtaining the water surface measurements. The flow was metered by a 1 inch orifice plate in a 2 inch supply line. Two and three dimensional models were tested with both smooth and rough boundaries. For the rough boundary tests, the bottom and the walls were lined with copper wire mesh of 16 meshes per inch.

The two dimensional semicircular models were constructed with diameters of 3, 4, and 5 inches. The material used was brass. The edges were machined to  $1/32$  of an inch and then beveled to a 45 degree angle. The two dimensional segment models were of the same type of construction as the semicircular models and had a value of  $\eta = d/r$  equal to 0.5 (see Figure 2b). The three dimensional semicircular models for the small flume were made of clear lucite. The length for all three dimensional models was 24 inches. The testing of segment arches was limited to the small flume only.



### Large Flume and Models

The majority of the tests reported here were performed in a larger 2 foot by 5 foot by 64 foot all steel tilting flume. The slope was controlled by six screw jacks driven by a common motor and gear reducer. The motor was operated by a raise, lower and stop switch. A revolution counter was attached at one end of the drive shaft and the actual slope of the flume bed was related to the number of revolutions and tenths of revolutions of the shaft. In this manner a change of slope with an accuracy of  $\pm 0.0000025$  foot/foot was easily accomplished in a matter of minutes. An 8 foot by 10 foot head box was equipped with an elliptical transition to provide a smooth change as the water flowed into the flume. The head box also contained several screens and one larger stone baffle. A skimming board which floated on the water surface prevented the propagation of surface waves in the flume. At the discharge end of the flume an adjustable sharp crested rectangular weir made of lucite was installed. A catchment box was made to eliminate any splash. The box discharged directly to the sump. The water was taken from a large recirculatory sump. One 2000 GPM pump and one 300 GPM pump fed the head box. The actual inflow was metered by two venturi's. The layout of the flume and the water supply system is shown in Figure 4.

An aluminum instrument carriage was mounted on adjustable stainless steel guide rails running the length of the flume. It was installed in such a manner that the flume bottom could be used as a reference plane. On the rack were mounted an electric point gage and a 1/4 inch Prandtl tube. The staff of the point gage was marked in millimeters and was equipped with a vernier which read to a tenth of a millimeter. The Prandtl tube was the type used normally for air. It was connected to an inverted U manometer which had a fluid of specific gravity 0.810. In addition a 50-tube piezometer stand was installed to obtain rapid

© 1997

100-100-100-100



measurements of the surface geometry. Fifty piezometer taps located at points along the centerline and 1 ft. and 2 ft. right and left of the centerline were hooked up to the piezometer bank. The bank was constructed so that it could be tilted to a 4.5 degree angle and was illuminated from the inside.

Sixteen models were used in the testing program. They were designed for specific values of  $b/B$  and  $L/b$ , where  $L$  is the length of the model measured in the direction of the flow. For a relative length ratio of  $L/b = 0$ , four models were made, one for each of the following values of  $M = b/B$ ;  $M = 0.3, 0.5, 0.7$ , and  $0.9$ . They were constructed with 1/2 inch marine plywood and faced with 22 gauge galvanized sheet metal. The three dimensional models were built with  $M$  values of  $0.3, 0.5, 0.7$ , and  $0.9$ . In each  $M$  group two models were constructed with  $L/b = 0.25$  and one model with  $L/b = 0.5$ . The basic construction was 1/2 inch marine plywood. The barrel was formed with galvanized sheet metal and one side of one of the  $L/b = 0.25$  models was faced with lucite. Figure 5 illustrates the three dimensional bridge models. Shown are the four models with  $L/b = 0.25$  and  $M = 0.3, 0.5, 0.7$ , and  $0.9$ . With this combination of models it was possible to test each of the openings  $M = 0.3, 0.5, 0.7$ , and  $0.9$  for relative lengths  $L/b$  of  $0, 0.25, 0.50, 0.75$ , and  $1.00$ . All of the models tested in the large flume were either two or three dimensional semi-circular models. The testing section was located between 20 and 50 feet from the entrance where it was possible to maintain uniform flow. In all cases the regain curve between sections 3 and 4 (Figure 1) was within the test section. In the great majority of the cases the boundary layer was fully developed within the first 20 feet of the flume, and fully developed uniform flow existed in the test section.

The actual testing program in the large flume was run under two different boundary roughness patterns. The first roughness which will be

1. The first part of the paper is devoted to a general discussion of the problem of the origin of life. It is shown that the problem is one of the most important and most difficult in the history of science.

2. The second part of the paper is devoted to a detailed discussion of the problem of the origin of life. It is shown that the problem is one of the most important and most difficult in the history of science. The paper is divided into two main parts. The first part is devoted to a general discussion of the problem of the origin of life. It is shown that the problem is one of the most important and most difficult in the history of science. The second part is devoted to a detailed discussion of the problem of the origin of life. It is shown that the problem is one of the most important and most difficult in the history of science.

referred to as the smooth boundary consisted of the steel flume walls being finished with an epoxy resin paint.

Manning's  $n$  for smooth boundaries had an average value of 0.0110. The range of  $n$  was from 0.009 to 0.0130 for discharges and Froude numbers from 1 cfs to 4 cfs and 0.05 to 1.00 respectively.

For the rough boundaries, the following roughness pattern was selected. Along the bottom of the flume, two layers of 1/4 inch aluminum rods were placed; a bottom layer of longitudinal bars placed 12 inches on center, and a top layer of transverse bars 6 inches on center. Along the sidewalls one layer of vertical bars 6 inches on center was placed 1/4 inch from the wall. The bottom layers of bars were tied together with wire. The vertical bars were tied at the bottom to the transverse bars and clamped to the wall above the free surface. The value of Manning's  $n$  for the rough boundaries ranged from 0.022 to 0.025 for discharges from 1 to 3 cfs and slopes from 0.000010 to 0.00450. The average value of  $n$  of 72 uniform flow tests was 0.0238.

### Tests

Seventy tests were run in the large flume with smooth boundaries covering a range of discharges from 1 to 2.5 cfs and a channel width ratio  $M$  varying from 0.3 to 0.9. One hundred and sixty eight tests were made in the large flume with rough boundaries for the conditions summarized in the table below, where the X's indicate the selected normal depth conditions for each of which the following values of  $M$  and  $L/b$ :

For  $M = b/B = 0.3, 0.5, 0.7, 0.9$

and  $L/b = 0.0, 0.5, 1.0$

Flow Rate	Froude Number													
	0.05	1.10	0.15	0.20	0.25	0.30	0.35	0.40	0.45	0.50	0.60	0.70	0.80	0.90
1 cfs	X			X	X		X	X		X	X		X	X
2 cfs		X	X		X			X			X	X		X
3 cfs			X			X			X			X		



Also with rough boundaries additional tests were made to establish that the expansion of the flow downstream from the minimum depth (profile between points 3 and 4 of Figure b) was complete and within the limits of the test section. A detailed surface topography was measured for  $Q = 1$  cfs, slope = 0.00584,  $M = 0.5$  and  $L/b = 0$ . Sufficient velocity profiles were taken at these conditions to plot isovel diagrams for the sections of uniform depth, maximum depth, vena contracta and the minimum depth. The isovel diagrams were also obtained for uniform flow corresponding to the following conditions:

$Q = 1$  cfs; slope = 0.004080

$Q = 2$  cfs; slope = 0.000131

The particular measurements that were taken on each of the smooth and rough boundary tests in the large flume were those required to calculate the following quantities: the hydraulic radius, the Reynolds number, the Froude number, the Darcy-Weisbach friction factor, the channel opening ratio  $M'$ , the discharge coefficient, the backwater ratio ( $y_1/y_n$ ), the backwater superslevation ( $h_1^*$ ), the surface profile ratio ( $h_1^*/\Delta h$ ), the length to the maximum backwater ( $L_{1-2}$ ), the length to the point of minimum depth ( $L_{2-3}$ ), the length  $L_{1-3}$ , and Manning's  $n$ . (See Figure 1 for the definition of terms). In view of the large amount of data that was to be analyzed and the repetitive character of the calculations, a program was prepared for processing the data on the Royal McBee LGP-30 digital computer.

The tabulation of the test data may be found in reference (17)\*\*.

#### ANALYSIS OF TEST RESULTS

##### Large Flume Smooth Boundary Model Tests

The experimental results of the two dimensional, semicircular, arch model tests in the large flume with smooth boundaries were plotted

---

\*\* A copy has been deposited at the Engineering Societies Libraries.



as the backwater ratio  $y_1/y_n$  vs the channel opening ratio  $M^0$  with the normal depth Froude number  $F_n$  as the parameter. This plot is shown in Figure 6a. As expected, the ratio of  $y_1/y_n$  decreased to unity for all Froude numbers as the value of  $M^0$  approaches 1.00. Also, it increases as  $M^0$  decreases. In a similar manner, the discharge coefficient  $C_d$  was plotted vs  $M^0$  for  $F_n$  and is shown in Figure 6b. As discussed in the theoretical analysis, the value of  $C_d$  tends to 0.611 at  $M^0 = 0$  and approaches the same value as the parameter  $F_n$  when  $M^0 = 1$ . The curves of Figure 6a and 6b have been interpolated for constant Froude numbers. The data was plotted on a large sheet of graph paper such that the Froude number for each data point could be identified. The points were then interpolated to obtain the constant parameter lines. This method was used to obtain all of the curves in which the Froude number appeared as the parameter.

### Large Flume Rough Boundary Model Tests

#### Backwater Ratio and Discharge Coefficient

The backwater ratio is plotted vs the channel opening ratio with the normal depth Froude number as the parameter for the two dimensional semicircular arch models as observed in the large flume with rough boundaries. In view of the importance of these curves, the scale was expanded and the results are shown in two parts. Figure 7a gives the results of  $y_1/y_n$  vs  $M^0$  for the range of backwater ratios less than 1.50. For the ratios greater than 1.50, Figure 7b should be used.

The experimental values of the discharge coefficient for the same test conditions are presented in Figure 8. This figure and Figures 7a and 7b have also been interpolated for constant Froude numbers.





### Location of the Points of Maximum Backwater, and Minimum Depth

In order to describe the centerline profile it is desirable to have an estimate of the distance from the upstream face of the constriction to the point of maximum backwater elevation. This distance is referred to as  $L_{1-2}$ . Because of the flatness of the surface profile in the vicinity of the maximum point, it was extremely difficult to get an exact measurement of  $L_{1-2}$ . The actual measurements taken could have been in error by as much as  $\pm 0.5$  feet. However, with the large amount of data which was available, it was possible to study  $L_{1-2}$  on an average basis. Average values of  $L_{1-2}$  were calculated for several combinations of  $b/B$ ,  $L/b$ ,  $L/B$ , etc. In this manner, it appeared that the effect of the variable bridge length and the change in  $M$  were of the same order to magnitude as the experimental error. The most consistent relationship was found by plotting the dimensionless ratio  $L_{1-2}/b$  vs the Froude number  $F_n$  with  $M = b/B$  as the parameter. This relationship is shown in Figure 9a. The values of  $L_{1-2}$  obtained from the smooth boundary tests also compared favorably with Figure 9a. In a similar manner it was found that the length  $L_{1-3}$  (distance from the maximum depth point to the minimum depth points) varied only with the constriction geometry. The values of  $L_{1-3}/b$  are plotted vs  $M = b/B$  with  $L/b$  as a parameter in Figure 9b. These curves are good for both two and three dimensional semicircular arch bridges.

### Determination of the Minimum Depth

Several other investigators have used the Froude number at section 3 ( $F_3 = V_3 / \sqrt{g Y_3}$ , see Figure 1) as an estimator of the maximum backwater. Others have used  $F_3$  as a controlling parameter in making indirect measurements of flood discharges. Due to the extremely irregular flow pattern at the minimum point, it would seem that the use of  $F_3$  may be misleading. In the present research, the normal depth Froude number  $F_n$  was found to be



a very reliable estimator of  $y_1/y_n$ . In order to test the variability of  $F_3$  with  $F_n$ , a correlation curve of  $F_3/F_n$  vs  $F_n$  was prepared. This curve is shown in Figure 10. Below a Froude number  $F_n$  of 0.5, the correlation was good. However, above  $F_n = 0.5$ , the depth  $y_3$  was often below the critical depth and the correlation of  $F_3/F_n$  to  $F_n$  was very poor. The scatter seemed to increase with increasing values of  $L/b$ . Therefore only the test results of the  $L/b = 0$  tests are shown. If used with caution, these curves can be used to estimate the minimum depth  $y_3$ . It appears from this curve that  $F_n$  is a much more reliable parameter than  $F_3$ .

#### Comparisons of Roughness Effects

Comparisons between the model tests in the smooth and rough channel were made by plotting the backwater ratio and the discharge coefficient against the normal depth Froude number  $F_n$  for constant channel opening ratios.

It appeared that the values are essentially the same for both smooth and rough conditions at Froude numbers  $F_n$  less than 0.5. Since the practical range of Froude numbers for natural channels is that less than 0.5, these curves show that for all practical purposes the effect of roughness can be ignored.

#### Comparison of Bridge Length Effects

Similarly, all of the  $L/b$  results were compared at constant values of the channel opening ratio  $M^0$ . Again it appears from the plots that <sup>for</sup> the practical range of field conditions, ( $L/b \leq 1.0$  and  $F_n \leq 0.5$ ) the effect of bridge length is negligible. The effect of length did seem to increase with a decrease in the channel opening ratio. However, as the value of  $M^0$  gets small, the physical properties are closer to those of a culvert rather than a bridge opening.

1. The first part of the report  
describes the general situation  
of the country and the  
state of the economy.

2. The second part of the report  
describes the state of the  
economy and the state of the  
country.

3. The third part of the report  
describes the state of the  
country and the state of the  
economy.

### Surface Topography and Velocity Diagrams

In order to complete the analysis of the maximum backwater, additional studies were made on the velocity distributions and the surface profiles. The studies were made for the condition of a sharp-crested semicircular constriction with  $M = b/B = 0.5$  and  $F_n$  approximately 0.20.

A detail of the surface topography both upstream and downstream of the model was observed. The result of this study is shown in Figure 11. The numbers shown indicate the depths in centimeters. Only a detail of one half of the surface is given since the pattern is essentially symmetrical. The graph shows lines of equal surface elevations. The centerline profile is also given in the figure. It is interesting to note that the actual maximum water surface elevation is not along the centerline, but on the upstream face of the abutment. This may be expected, since there is a stagnation point at the abutment. The actual rise in elevation is equivalent to the velocity head of approach. Field measurements indicate that this pile-up does not occur in actual conditions and therefore it is assumed to be of no consequence in the application of the results to field conditions.

Several velocity profiles were taken in the large flume with rough boundaries. Traverses were run with the Prandtl Tube at four sections with the  $M = 0.5$ ,  $L/b = 0.0$  and  $F_n$  approximately 0.20 model tests. The first section was in the normal depth flow without the model. The second was at the section of maximum backwater, the third at the vena contracta and the fourth at the section of minimum depth. Plots of equal velocity lines were prepared for each section. A composite picture of the isovel diagrams is shown in Figure 12. Only half of the diagrams is given due to symmetry. The discharge obtained by integration of the velocity diagrams



checked that measured with the venturi meter within 1%.

In addition isovel diagrams were obtained for two other uniform flow conditions. From these diagrams and from Figure 12a, the following values of the kinetic energy correction factor and the momentum correction factor were obtained for uniform flow conditions:

Q	Slope	$y_{11}$	Approx. $F_n$	$\alpha$	$\beta$
2 cfs	0.000131	0.799 ft.	0.10	1.145	1.055
1 cfs	0.000584	0.319 ft.	0.20	1.216	1.084
1 cfs	0.004080	0.173 ft.	0.50	1.250	1.090

Based upon a centerline velocity profile for  $Q = 3.714$  cfs and  $S=0.0125$  the value of  $\alpha$  was determined as 1.01. This value, based on an assumed two dimensional flow, is less than that of 1.145, 1.216 and 1.250 determined from the integration of the isovel diagrams which took into account the effects of the sides and corners. Other investigators have assumed that  $\alpha$  is unity for a rigid rectangular flume. This calculation verifies that this assumption is correct if the flow is nearly two dimensional.

#### THE GENERALIZED BACKWATER EQUATION

With the introduction of the channel opening ratio  $M'$ , the assumption was made that the backwater produced by constrictions of the same  $M'$  would be equal regardless of the physical geometry of the actual constriction. In order to verify this assumption, test data on constriction geometries other than a semicircle was needed.

A series of 93 tests were run by A. A. Socky in the small flume on two dimensional segment weirs with a  $\eta = d/r$  value of 0.5. (see Figure 2). The data obtained were analyzed in terms of  $M'$ . These tests were run in the small channel with rough boundaries which had a Manning's  $n$  of 0.0201. Results were plotted in the same manner as for the large flume





rough tests and are shown in Figure 13. When compared to the large flume results of Figure 7, the values of the backwater ratio for a given  $F_n$  and  $M^0$  are almost identical. In spite of the fact that each set of curves had been interpolated, the small differences could easily be attributed to experimental and graphical error.

In a similar manner, the vertical canal data given by Liu<sup>6</sup> was reanalyzed to fit the  $y_1/y_n$  vs  $M^0$  method of presentation. These tests were run in a wider flume with a different roughness pattern. Their roughness produced a Manning  $n$  of 0.024. The results were compared to the semi-circular data given previously and to the segment data. Again the differences were extremely small and attributable to experimental error. It is extremely interesting to note that the test data taken by three investigators in three different flumes and under three completely different constriction geometries produced almost identical results. This clearly verifies that the channel opening ratio  $M^0$  is a governing variable. Of course, the data compared were those in which the eccentricity was zero, the skew was zero, and the entrance was sharp.

It would seem that due to the similarity of the results there should be a common relationship between the backwater ratio  $y_1/y_n$ , the Froude number  $F_n$  and the channel opening ratio  $M^0$  which would fit all of the data. This relationship should then be applicable to all constriction geometries. As mentioned previously in the analysis, a similarity was noticed between the several different backwater equations. The term  $(F_n/M^0)^{2/3}$  appeared in all of the solutions of  $y_1/y_n$ . In general, it appeared that

$$y_1 / y_n = C \left[ (F_n / M^0)^{2/3} \right]^d \quad \text{---(2E)}$$

The first part of the paper is devoted to a study of the properties of the function  $f(x)$  which is defined by the equation  $f(x) = \int_0^x f(t) dt$ . It is shown that  $f(x)$  is a continuous function and that it satisfies the differential equation  $f'(x) = f(x)$ . The second part of the paper is devoted to a study of the properties of the function  $g(x)$  which is defined by the equation  $g(x) = \int_0^x g(t) dt$ . It is shown that  $g(x)$  is a continuous function and that it satisfies the differential equation  $g'(x) = g(x)$ . The third part of the paper is devoted to a study of the properties of the function  $h(x)$  which is defined by the equation  $h(x) = \int_0^x h(t) dt$ . It is shown that  $h(x)$  is a continuous function and that it satisfies the differential equation  $h'(x) = h(x)$ .

The fourth part of the paper is devoted to a study of the properties of the function  $i(x)$  which is defined by the equation  $i(x) = \int_0^x i(t) dt$ . It is shown that  $i(x)$  is a continuous function and that it satisfies the differential equation  $i'(x) = i(x)$ . The fifth part of the paper is devoted to a study of the properties of the function  $j(x)$  which is defined by the equation  $j(x) = \int_0^x j(t) dt$ . It is shown that  $j(x)$  is a continuous function and that it satisfies the differential equation  $j'(x) = j(x)$ . The sixth part of the paper is devoted to a study of the properties of the function  $k(x)$  which is defined by the equation  $k(x) = \int_0^x k(t) dt$ . It is shown that  $k(x)$  is a continuous function and that it satisfies the differential equation  $k'(x) = k(x)$ .

The seventh part of the paper is devoted to a study of the properties of the function  $l(x)$  which is defined by the equation  $l(x) = \int_0^x l(t) dt$ . It is shown that  $l(x)$  is a continuous function and that it satisfies the differential equation  $l'(x) = l(x)$ . The eighth part of the paper is devoted to a study of the properties of the function  $m(x)$  which is defined by the equation  $m(x) = \int_0^x m(t) dt$ . It is shown that  $m(x)$  is a continuous function and that it satisfies the differential equation  $m'(x) = m(x)$ .

where C is a coefficient which would take into account the effects of the discharge coefficient, approach velocity, and non-uniform velocity distributions and other empirically determined factors. Equation (28) is actually the equation of a straight line on logarithmic paper with a slope of  $\frac{1}{3}$ . A total of 50 semicircular  $L/b = 0$  test values, 44 vertical board values (Colorado) and 50 segment values was plotted in the form of  $y_1/y_n = 1$  vs  $(F_n/M^3)^{2/3}$  and is shown in Figure 14. The value of  $y_1/y_n = 1$  was used in order to expand the scale of the backwater ratio. It is quite apparent that the data tend to collapse into one straight line relationship.

The method of least squares was applied to a random sample of the 144 test points to determine the empirical straight line relationship. After solving for  $\frac{1}{3}$  and C, equation (28) became

$$y_1 / y_n = 1 + 0.47 \left[ (F / M^3)^{2/3} \right]^{3.33} \quad \text{---(29)}$$

Equation (29) is a very simple and easy solution for the backwater produced by any type of constriction. In actual practice, this equation will give as good an estimate of the maximum backwater  $y_1$  as any previously suggested method.

It has been suggested by C. F. Izzard that equation (29) could be approximated by

$$y_1 / y_n = 1 + 0.45 (F / M^3)^2 \quad \text{---(30)}$$

and still fit the data very closely.



## MODEL-PROTOTYPE COMPARISON AND DESIGN PROCEDURES

The most important variables in determining the maximum backwater are the normal depth Froude number  $F_n$  and the channel opening ratio  $M^0$ . As defined,  $M^0$  can be used for any type of bridge geometry. The boundary roughness and the bridge length for Froude numbers less than 0.5 are relatively unimportant and their effects for all practical purposes can be neglected. In analyzing a field situation, difficulty sometime arises in defining the normal depth and the normal depth Froude number for an irregular natural channel. The normal depth Froude number for an irregular natural channel. The normal hydraulic depth of  $y_n$  should be taken as  $A_n/B_n$ , where  $A_n$  is the uniform flow cross sectional area and  $B_n$  is the uniform flow surface width. The Froude number is defined as

$$F_n = V_n / \sqrt{g y_n / \alpha} = \sqrt{(Q^2 B_n / A_n^3 g) / \alpha} \quad \text{---(31)}$$

For  $\alpha = 1$  reduces to

$$F_n = V_n / \sqrt{g y_n} = \sqrt{Q^2 B_n / A_n^3 g} \quad \text{---(32)}$$

For prototype calculation the last expression in (31) or (32) is recommended. The effect of the kinetic energy correction factor  $\alpha$  on the Froude number, may be evaluated from the velocity distributions. It is customarily assumed that the incorporation of the kinetic energy correction factor  $\alpha$  into the field calculations would account for a portion of the differences between model and prototype. This can be done in the following way. For similarity it is necessary that

$$\begin{aligned} (V / \sqrt{g y_n / \alpha})_{\text{model}} &= (\sqrt{Q^2 B_n / A_n^3 g / \alpha})_{\text{prototype}} \\ \text{or} \\ (V / \sqrt{g y_n})_{\text{model}} &= (\sqrt{Q^2 B_n / A_n^3 g})_{\text{prototype}} \sqrt{(\alpha_p / \alpha_m)} \end{aligned} \quad \text{---(33)}$$



When  $\alpha_p$  is approximately equal to  $\alpha_m$  the effect of the kinetic energy coefficient may be neglected. In actual natural streams it is of the order of 1.25 which is very close to the present experimental values. In what follows, the ratio of  $(\alpha_p / \alpha_m)^{1/2}$  is taken as unity. However, its effect could be evaluated by means of equation (33).

### Design Procedures

The best experimental approximation to the backwater ratio for semicircular arch bridges without skew, eccentricity or entrance rounding is given by figures 7a and 7b. Equation (23) could be used to calculate  $y_1 / y_n$  by obtaining the discharge coefficient from Figure 8. A more practical first approximation to the maximum backwater is given by the curves of Figure 14 or by equation (29) or (30).

### Indirect Discharge Measurement

If the concepts presented in this paper are used as a method for making indirect estimations of flood discharges, the following detailed procedure is recommended. The steps outlined provide an estimation and not a direct calculation.

#### A. Preliminary Computations

- 1.) Obtain from a field survey a cross-section view of the stream at the approach section (section at the maximum backwater elevation) and at the upstream face of the bridge.
- 2.) For several elevations determine the area below that elevation for each section. This is most readily accomplished by plotting the section views to a fairly large scale and using an area planimeter to obtain the respective areas. Also for each elevation, determine the surface widths at the approach section.

1. The first part of the paper is devoted to a general discussion of the problem of the existence of solutions of the system of equations (1) for arbitrary values of the parameters  $\alpha$  and  $\beta$ . It is shown that the system has solutions for arbitrary values of the parameters  $\alpha$  and  $\beta$  if and only if the condition  $\alpha + \beta = 1$  is satisfied.

2. The second part of the paper is devoted to a detailed analysis of the case  $\alpha = 0$  and  $\beta = 1$ . It is shown that in this case the system has solutions for arbitrary values of the parameters  $\alpha$  and  $\beta$  if and only if the condition  $\alpha + \beta = 1$  is satisfied.

3. The third part of the paper is devoted to a detailed analysis of the case  $\alpha = 1$  and  $\beta = 0$ . It is shown that in this case the system has solutions for arbitrary values of the parameters  $\alpha$  and  $\beta$  if and only if the condition  $\alpha + \beta = 1$  is satisfied.



- 3.) With the respective elevations, areas, and surface widths plot the four working curves shown in Figure 15.

B. Trial and Error Solution for the Discharge

- 1.) From the survey of high water marks, obtain the maximum surface elevation for the given flood.
- 2.) Enter curve (3) with this elevation and obtain the maximum surface width  $B_1$  (max.).
- 3.) With  $B_1$  (max.) enter curve (4) and obtain  $y_1$  (max.) (the maximum hydraulic depth.)
- 4.) Assume a value of the normal hydraulic depth  $y_n$  ( $y_n < y_1$ ).
- 5.) With  $y_n = A/B$  get the assumed normal depth surface width  $B_{n1}$  from curve (4).
- 6.) Enter curve (3) with  $B_{n1}$  and obtain the corresponding elevation.
- 7.) With this elevation obtain the value of the channel opening ratio  $M^0 = A_{n2}/A_{n1}$  and the normal depth approach area  $A_{n1}$  from curves (2) and (1) respectively.
- 8.) Compute  $y_1/y_n$  and obtain the normal depth Froude number from equation (29).
- 9.) With the Froude number  $F_n$  defined as equation (32), calculate the discharge  $Q_c$ . This will give a first estimate of the flood discharge.
- 10.) With  $M^0$  and  $F_n$  go to Figure 3 and obtain the discharge coefficient  $C_d$ .
- 11.) As a second estimate, compute the discharge according to equation (15), where  $b$  is the distance between abutments at the springline of the arch,  $r$  is the radius of curvature of the arch, and  $y_1$  is the distance from the maximum water

2) With the same  
place the four walls

3) ... and ...  
... the ...  
... the ...

...  
...  
...  
...

...  
...  
...  
...

...  
...  
...  
...

...  
...  
...  
...

...  
...  
...  
...

surface elevation to the average bottom at the bridge section. The average bottom depth is computed as the ratio of the area below the springline of the arch to the distance between abutments.

- 12.) If the discharge is the same as computed by step 1 of part B then the estimate is completed. If they are not equal, another  $Y_1$  should be chosen in step 1, and the process repeated until the two discharge calculations are equal.

The design procedure has been used for model-prototype comparison of the discharge for the Crooked Creek Flood at Madison, Indiana on January 24, 1976.

#### Determination of Location / Approximation

For determining the location for a given discharge predicted by a new design span, semicircular arch bridge where the springline of the arch is on the bed of the stream, the following design procedure is recommended. It must be emphasized again that the restrictions of no skew, no eccentricity and no entrance standing should be observed.

- 1.) If stage-discharge records are available, plot the normal depth or a section view of the stream cross-section where the bridge is to be built. This elevation should correspond to the elevation of the design flood water surface.
- 2.) Superimpose the proposed bridge profile on the section view.
- 3.) Determine the value of  $M = b/8$ .
- 4.) Calculate  $Y_1/r$  and obtain the value of  $C_M$  from figure 5 for the curve of  $\eta = 0$ . When the center of curvature



is below the springline of the arch, calculate  $\Delta z$  and use the respective  $\eta$  curve to obtain  $\eta$ .

5. Calculate the normal depth  $D_n$  from the equation (22).

6. Calculate  $\Delta z = H - D_n$ .

7. From the  $\Delta z$   $\eta_{H, \Delta z}$  use the  $\eta_{H, \Delta z}$  curve from Figure 10 to get the  $\eta_{H, \Delta z}$  value. Use the calculated  $\eta_{H, \Delta z}$  and  $D_n$  to get  $\eta$  from (20).

8. Use  $\eta_{H, \Delta z}$  and  $\eta$  to get  $\eta_{H, \Delta z}$  from Figure 11 to get  $\eta_{H, \Delta z}$  value. Use  $\eta_{H, \Delta z}$  and  $D_n$  to get  $\eta$  from (20).

9. Use  $\eta_{H, \Delta z}$  and  $\eta$  to get  $\eta_{H, \Delta z}$  from Figure 11 to get  $\eta_{H, \Delta z}$  value. Use  $\eta_{H, \Delta z}$  and  $D_n$  to get  $\eta$  from (20).

10. Calculate  $\Delta z = H - D_n$  from (20).

11. Use the  $\Delta z$   $\eta_{H, \Delta z}$  use the  $\eta_{H, \Delta z}$  curve from Figure 10 to get the  $\eta_{H, \Delta z}$  value.

12. Use the  $\Delta z$   $\eta_{H, \Delta z}$  use the  $\eta_{H, \Delta z}$  curve from Figure 10 to get the  $\eta_{H, \Delta z}$  value. Use the  $\Delta z$   $\eta_{H, \Delta z}$  use the  $\eta_{H, \Delta z}$  curve from Figure 10 to get the  $\eta_{H, \Delta z}$  value.

13. Use the  $\Delta z$   $\eta_{H, \Delta z}$  use the  $\eta_{H, \Delta z}$  curve from Figure 10 to get the  $\eta_{H, \Delta z}$  value. Use the  $\Delta z$   $\eta_{H, \Delta z}$  use the  $\eta_{H, \Delta z}$  curve from Figure 10 to get the  $\eta_{H, \Delta z}$  value.

14. Use the  $\Delta z$   $\eta_{H, \Delta z}$  use the  $\eta_{H, \Delta z}$  curve from Figure 10 to get the  $\eta_{H, \Delta z}$  value. Use the  $\Delta z$   $\eta_{H, \Delta z}$  use the  $\eta_{H, \Delta z}$  curve from Figure 10 to get the  $\eta_{H, \Delta z}$  value.

15. Use the  $\Delta z$   $\eta_{H, \Delta z}$  use the  $\eta_{H, \Delta z}$  curve from Figure 10 to get the  $\eta_{H, \Delta z}$  value. Use the  $\Delta z$   $\eta_{H, \Delta z}$  use the  $\eta_{H, \Delta z}$  curve from Figure 10 to get the  $\eta_{H, \Delta z}$  value.

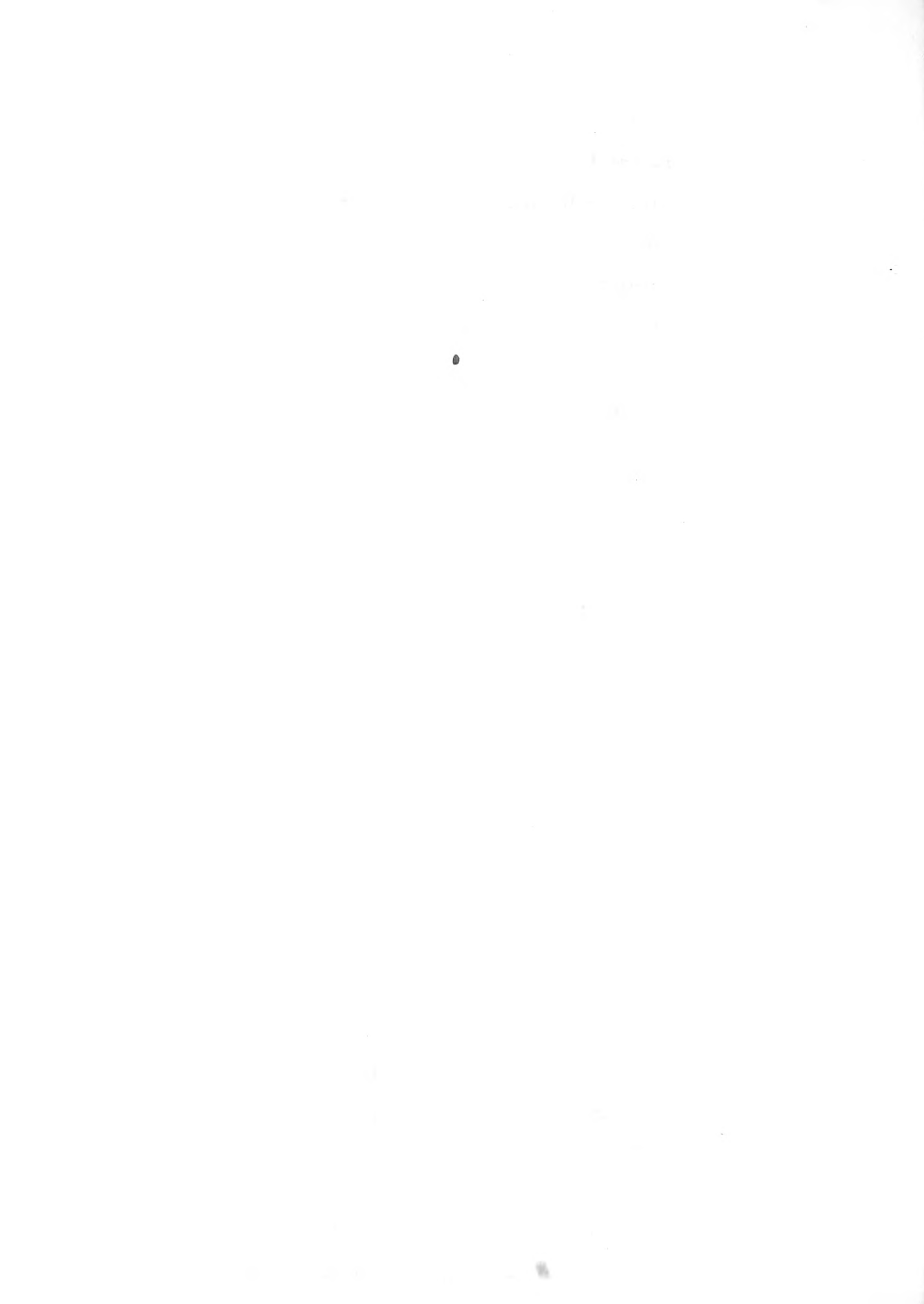
16. Use the  $\Delta z$   $\eta_{H, \Delta z}$  use the  $\eta_{H, \Delta z}$  curve from Figure 10 to get the  $\eta_{H, \Delta z}$  value. Use the  $\Delta z$   $\eta_{H, \Delta z}$  use the  $\eta_{H, \Delta z}$  curve from Figure 10 to get the  $\eta_{H, \Delta z}$  value. Use the  $\Delta z$   $\eta_{H, \Delta z}$  use the  $\eta_{H, \Delta z}$  curve from Figure 10 to get the  $\eta_{H, \Delta z}$  value.

17. Calculate the backwater ratio  $\eta_{H, \Delta z}$  where  $\eta_{H, \Delta z}$  is the hydraulic depth corresponding to the given permissible maximum water surface.

18. Calculate the backwater ratio  $\eta_{H, \Delta z}$  where  $\eta_{H, \Delta z}$  is the hydraulic depth corresponding to the given permissible maximum water surface.

19. Obtain  $\eta_{H, \Delta z}$  and  $B_{H, \Delta z}$  from this section view for the maximum permissible backwater elevation. Obtain the normal depth  $D_n$  from Figure 10.

20. Obtain  $\eta_{H, \Delta z}$  and  $B_{H, \Delta z}$  from this section view for the maximum permissible backwater elevation. Obtain the normal depth  $D_n$  from Figure 10.



- 5.) With  $y_1/x_1$  and  $R_1$  calculate the channel opening ratio from equation (29).
- 6.) With  $M$  and  $A_{n-1}$  compute the required minimum normal depth area ( $A_n$ ) as  $A_{n2} = 1.1 A_{n1}$ .
- 7.) Adjust the span width, radius of curvature and the depth to the center of curvature to fit the required minimum area  $A_{n2}$ .

Example: Flood of January 21, 1959 at Madison, Indiana.

The model-prototype comparison is done according to the design procedure recommended for estimating flood discharges at arch bridge contractions. The field survey data is part of a report on the indirect estimation of floods by the office of the U. S. Geological Survey in Indianapolis, Indiana. The flood under study is one that occurred on January 21, 1959 in the Crooked Creek at Madison, Indiana. Following the procedure which was outlined by Kindsvater, Carter and Tracy in reference 5, the Survey estimated the flood to be 4200 cfs. Although the arch is essentially semicircular and without skew, the rather high degree of eccentricity and the extremely irregular channel section makes the present system of analysis somewhat doubtful. The value of the discharge obtained by the proposed method was 4580 cfs. or about 9% larger than that calculated by the U.S.G.S.





## CONCLUSIONS

Testing of circular arch constriction models with no skew, no eccentricity and no entrance rounding was made. It was found that the parameters governing the backwater ratio and the discharge coefficient are the Froude number of the approaching flow  $F_n$  and the channel opening ratio  $M^2$ . The bridge length and channel roughness effects are negligible for Froude numbers less than 0.5. A generalized relationship between the backwater ratio, the Froude number and the channel opening ratio (equ. 29) was found to hold for geometries other than circular arches. Design procedures are suggested for indirect discharge measurement, determination of backwater superelevation, and determination of required waterway area. These procedures make use of figures 7, 8, 9, 10, and 14, which are tentatively recommended as design curves.



#### ACKNOWLEDGMENT

This research was sponsored by the State Highway Department of Indiana in cooperation with the U. S. Department of Commerce, Bureau of Public Roads. The authors wish to express their appreciation to Mr. C. F. Izzard, Director of Hydraulic Research, U. S. Bureau of Public Roads, Washington, D. C., for his valuable comments and suggestions and to Mr. H. J. Owen, Associate Research Scientist, Illinois Water Resources Commission, Urbana, Illinois, who, while a Research Assistant at Purdue University, designed and supervised the construction of the large flume and started the model testing with smooth boundaries. Thanks are also given to Mr. A. A. Socky, Research Assistant at Purdue University, who performed the testing of segment arch models in the small flume.

1947-48

1948-49

1949-50

1950-51

1951-52

1952-53

1953-54

1954-55

1955-56

1956-57

# BIBLIOGRAPHY

1. Lane, E. W. "Experiments on the Flow of Water Through Contractions in Open Channels", Trans. ASCE, Vol. 57, 1910-20 pp. 1149-1211.
2. Kindsvater, C. E. and Carter, R. W. "Tranquil Flow Through Open-Channel Contractions", Trans. ASCE, Vol. 120, 1955, pp. 1055-1080.
3. Tracy, H. J. and Carter, R. W. "Backwater Effects of Open-Channel Contractions", Trans. ASCE, Vol. 120, 1955, pp. 991-1006.
4. Izard, C. F. Discussions on "Backwater Effects of Open-Channel Contractions" by H. J. Tracy and R. W. Carter, Trans. ASCE, Vol. 120, 1955, pp. 1008-1013.
5. Kindsvater, C. E., Carter, R. W. and Tracy, H. J. "Computation of Peak Discharge at Contractions", U.S.G.S. Open File #413, Washington, D. C., 1953.
6. Lin, H. T., Bradley, J. W. and Flato, W. J. "Backwater Effects of Piers and Abutments", Colorado State University, CER57-ML10, October, 1957.
7. Bradley, J. W. "Hydraulics of Bridge Waterways", U. S. Department of Commerce, Bureau of Public Roads, Washington, D. C., August 1960.
8. Vallentine, H. R. "Flow in Rectangular Channels with Lateral Constriction Places", La Houille Blanche, Jan.-Feb. 1953, pp. 75-84.
9. Herbich, J. B., Carls, R. A. and Kable, J. C. "The Effects of Spur Dikes on Flood Flows Through Highway Bridge Contractions", Fritz Engineering Laboratory, Lehigh University, June, 1959.
10. Owen, H. J., Socky, A. A., Husain, S. T., and Delleur, J. W. "Hydraulics of River Flow Under Arch Bridges - A Progress Report", Proceedings of the 45th Road School, Purdue Engineering Experiment Station, Series No. 100, March 1960.
11. Buckingham, E. "On Physically Similar Systems", Phys. Rev., Vol. 4, Ser. 2, pp. 345-376, 1931.
12. Streeter, V. L. "Fluid Dynamics", McGraw-Hill Book Co., New York, 1948, pp. 174-177.
13. Owen, H. J. "Design and Construction of a Hydraulic Testing Flume and Backwater Effects of Semicircular Contractions in a Smooth Rectangular Channel", Progress Report No. 2, Joint Highway Research Project, Purdue University, January, 1960.
14. Daugherty, R. L. and Ingersoll, A. C. "Fluid Mechanics", McGraw-Hill Book Co., New York, 1954.

12  
 13  
 14  
 15  
 16  
 17  
 18  
 19  
 20  
 21  
 22  
 23  
 24  
 25  
 26  
 27  
 28  
 29  
 30  
 31  
 32  
 33  
 34  
 35  
 36  
 37  
 38  
 39  
 40  
 41  
 42  
 43  
 44  
 45  
 46  
 47  
 48  
 49  
 50  
 51  
 52  
 53  
 54  
 55  
 56  
 57  
 58  
 59  
 60  
 61  
 62  
 63  
 64  
 65  
 66  
 67  
 68  
 69  
 70  
 71  
 72  
 73  
 74  
 75  
 76  
 77  
 78  
 79  
 80  
 81  
 82  
 83  
 84  
 85  
 86  
 87  
 88  
 89  
 90  
 91  
 92  
 93  
 94  
 95  
 96  
 97  
 98  
 99  
 100

15. Chow, V. T. "Open Channel Hydraulics", McGraw-Hill Book Co., New York, 1959
16. Henry, H. F. Discussion on "Diffusion of submerged jets", by Albertson, Dai, Jensen, and Rouse. Trans. ASCE, Vol. 115, 1950, pp 687-694.
17. Biery, P. M. and Delleur, J. W. "Hydraulics of Single Span Arch Bridge Constrictions", Report No. 8, Joint Highway Research Project No. C-36-623, School of Civil Engineering, Purdue University, Lafayette, Indiana.

12. Show that if  $f$  is a function from  $A$  to  $B$  and  $C$  is a subset of  $A$ , then  $f(C)$  is a subset of  $B$ .

13. Let  $f$  be a function from  $A$  to  $B$ . Show that  $f$  is injective if and only if for every subset  $C$  of  $A$ ,  $f(C)$  is a subset of  $B$ .

14. Let  $f$  be a function from  $A$  to  $B$ . Show that  $f$  is surjective if and only if for every subset  $C$  of  $B$ ,  $f^{-1}(C)$  is a subset of  $A$ .



# NOTATIONS

<u>SYMBOL</u>	<u>UNITS</u>	<u>DEFINITION</u>
A	$L^2$	Area
$A_{n1}$	$L^2$	Total normal depth flow area at section 1
$A_{n2}$	$L^2$	Normal depth flow area at section 2
a	L	Roughness height
B	L	Rectangular channel width or surface width for a non-rectangular channel
b	L	Span width at the springline of the arch
C		A coefficient
C	$L^{1/2}/T$	The Chezy roughness coefficient = $V_n/\sqrt{R_n S}$
$C_d$		Coefficient of discharge
$C_M$		Channel opening ratio coefficient
D	L	Hydraulic depth as defined by V. T. Chow
d	L	Depth of flow in a steep open channel
d	L	Distance from the springline to the center of curvature of the arch
F		Denotes a mathematical function
$F_n$		Normal depth Froude number = $V_n/\sqrt{gy_n}$
$F_3$		Froude number at the section of minimum depth
f		Denotes a mathematical function
f		Darcy-Weisbach friction factor
G		Denotes a mathematical function
g		Denotes a mathematical function
g	$L/T^2$	Acceleration of gravity
H	L	Total energy head

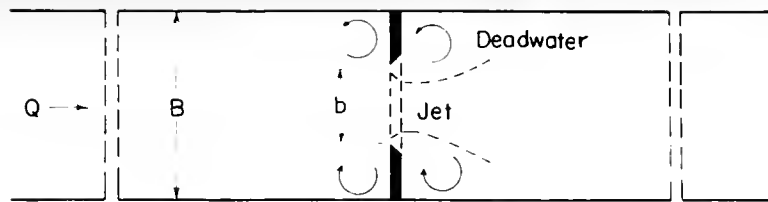


$h_1^*$	L	Backwater superelevation
$h$	L	Difference between the maximum and minimum surface elevations
$i$		Subscript denoting a subsection of an isovel diagram
$K$		Weir coefficient
$L$	L	Length of the bridge parallel to the direction of the flow
$L_{1-2}$	L	The distance along the centerline from the upstream face of the bridge to the maximum backwater elevation
$L_{2-3}$	L	The distance along the centerline from the upstream face of the bridge to the minimum surface elevation
$M$		Channel width ratio $b/B$
$M^v$		Channel opening ratio
$M_1$		Mild slope backwater curve in an open channel
$n$	$L^{1/6}$	Manning's roughness coefficient
$n$		Subscript which refers to the normal depth for uniform flow
$p$	$F/L^3$	Pressure
$Q$	$L^3/T$	Total flow
$q$	$L^3/T$	That portion of the total flow which could pass through the bridge without contraction
$R$	L	Hydraulic radius
$r$	L	Radius of curvature of the arch
$S$		Slope
$T$		An infinite series of powers of the ratio of the maximum depth to the radius of curvature

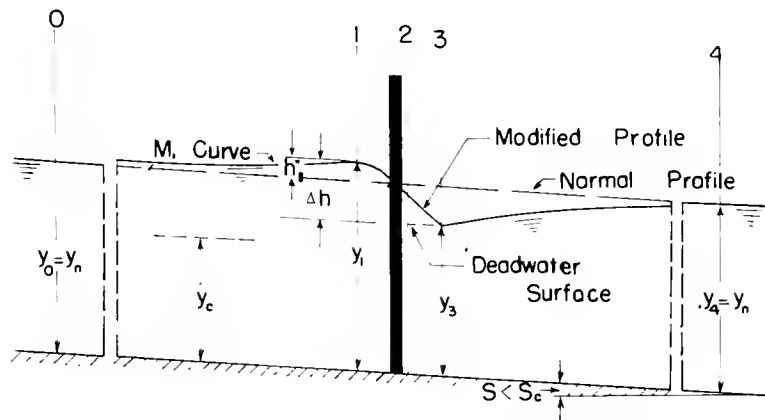


$V$	$L/T$	Average velocity
$v$	$L/T$	Local velocity
$y$	$L$	Depth of flow
$y_n$	$L$	Depth of the normal uncontracted flow
$y_1$	$L$	Depth of flow at the section of maximum backwater
$y_2$	$L$	Depth of flow at the vena contracts
$y_3$	$L$	Minimum depth of flow
$\alpha$		Kinetic energy coefficient
$\beta$		Momentum coefficient
$\gamma$	$F/L^3$	Specific weight of water
$\zeta$		Ratio of $y_n / r$
$\eta$		Ratio of $d / r$
$\nu$	$L^2/T$	Kinematic viscosity of the fluid
$\rho$	$Ft^2/L^4$	Fluid mass density





A.) PLAN



B.) MILD SLOPE CHANNEL

C.) WEIR PLATES

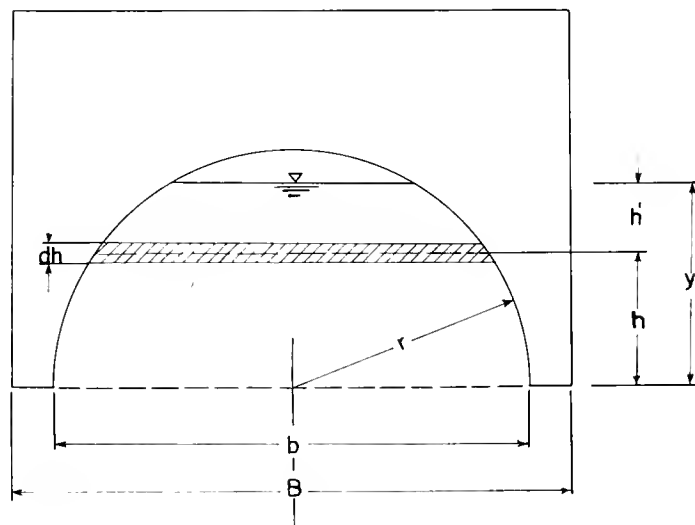
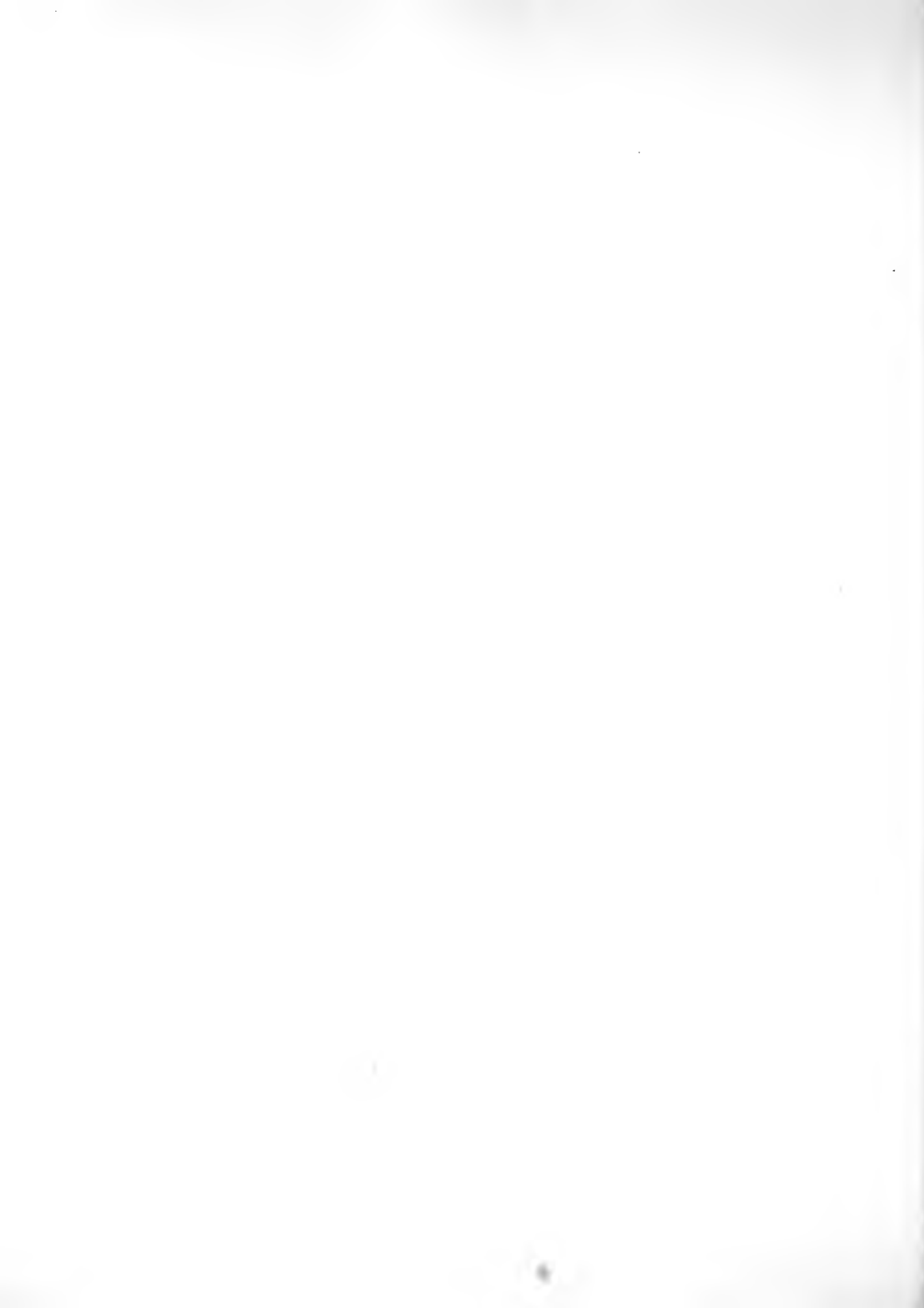
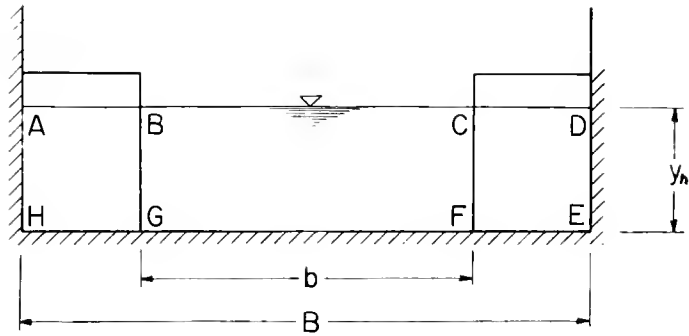


FIGURE I DEFINITION SKETCH





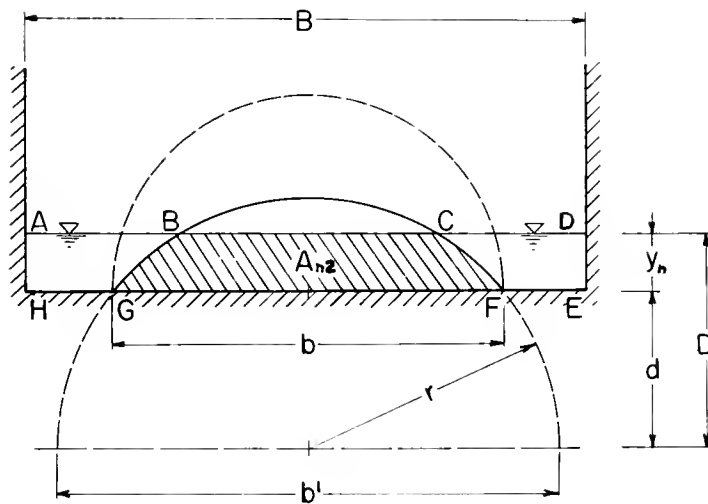
(a)



FLOW IN ADEH =  $Q = V_h B y_h$

FLOW IN BCFG =  $q = V_h b y_h$

(b)



FLOW IN ADEH =  $Q = V_h B y_h$

FLOW IN BCFG =  $q \neq V_h b y_h$

FIGURE 2 — DEFINITION SKETCH FOR THE DEVELOPMENT OF THE CHANNEL OPENING RATIO



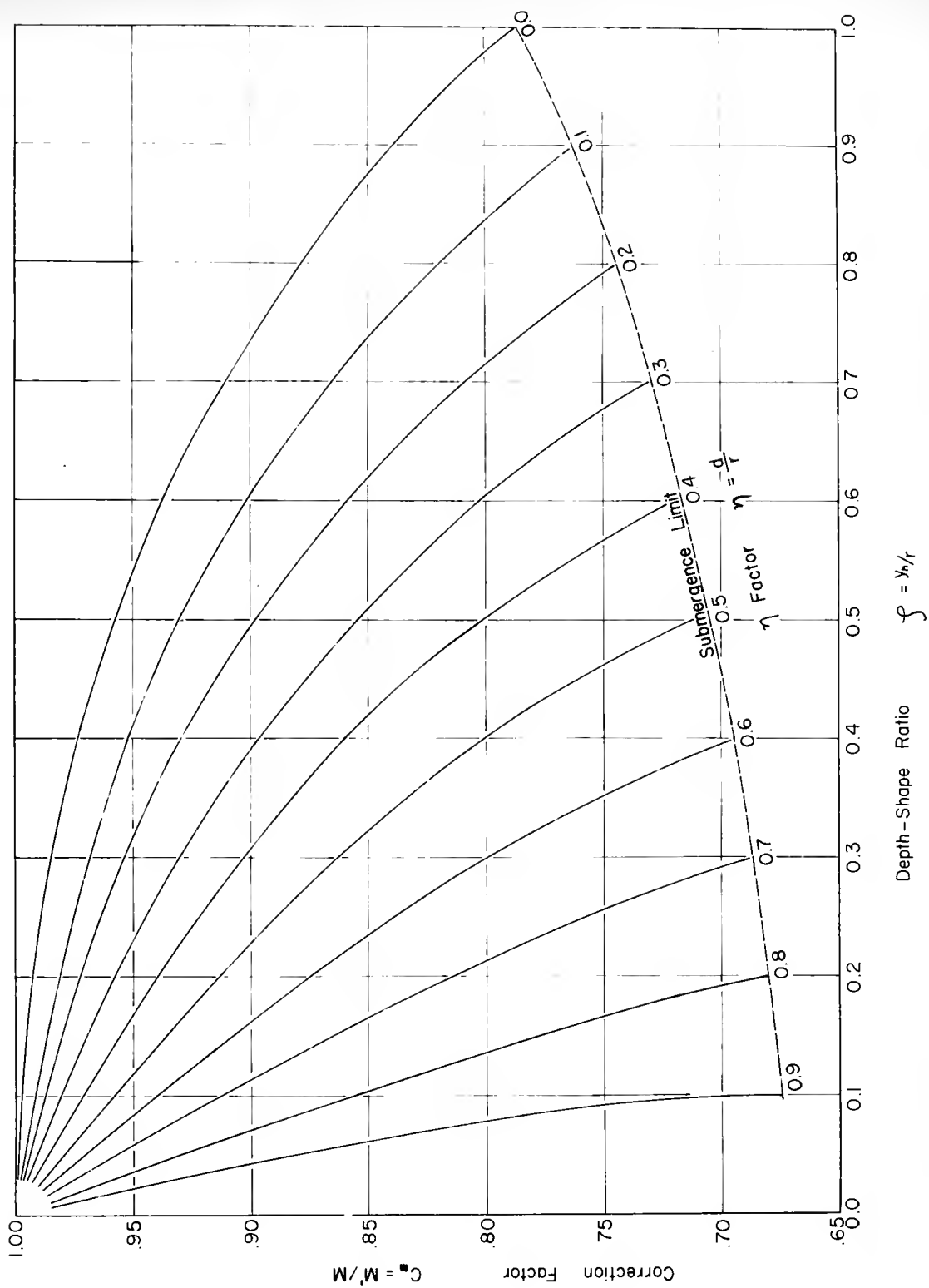


FIGURE 3 — CORRECTION COEFFICIENT FOR THE CHANNEL OPENING RATIO



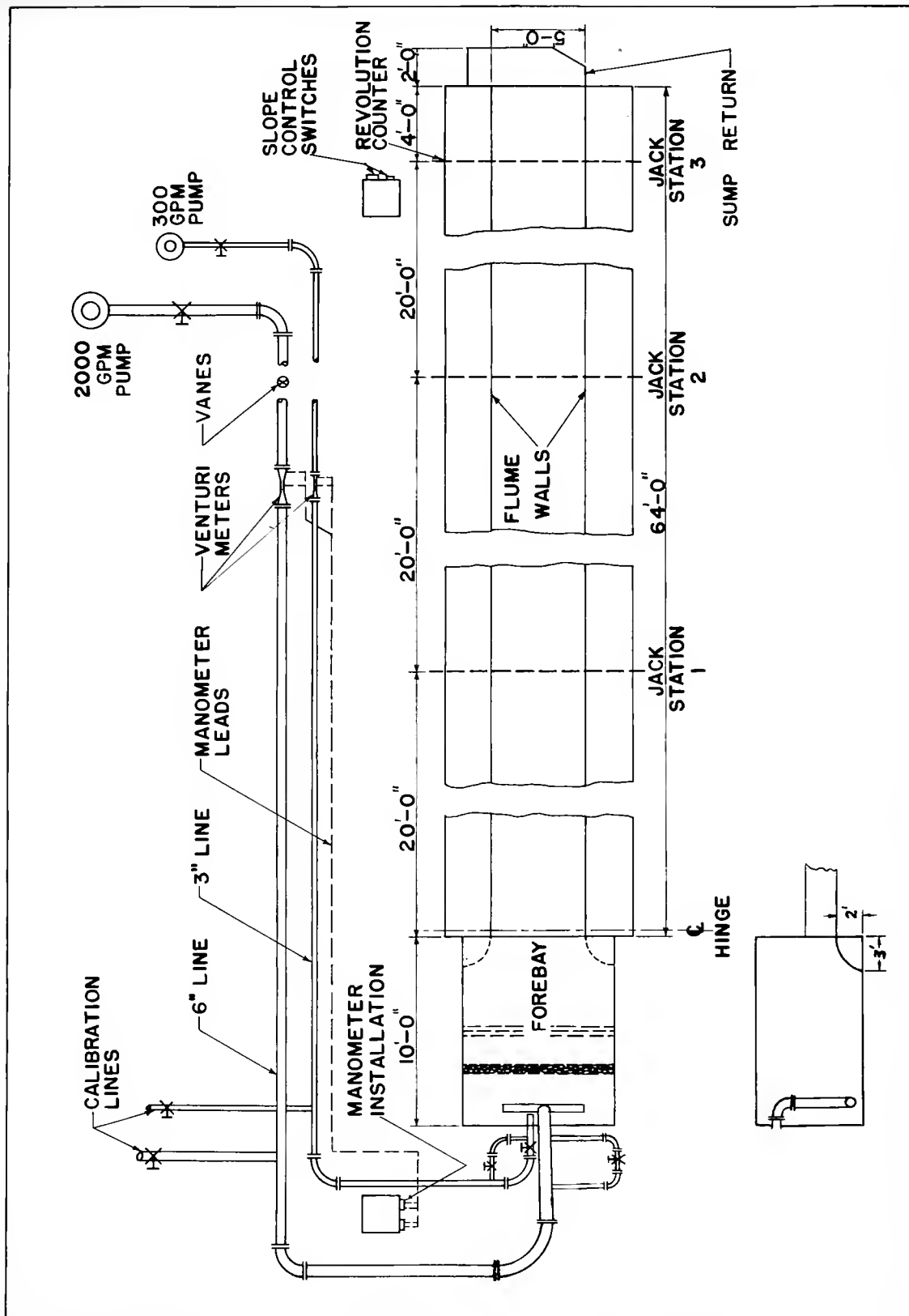


FIGURE 4 - APPARATUS ARRANGEMENT





FIG 5 MODELS





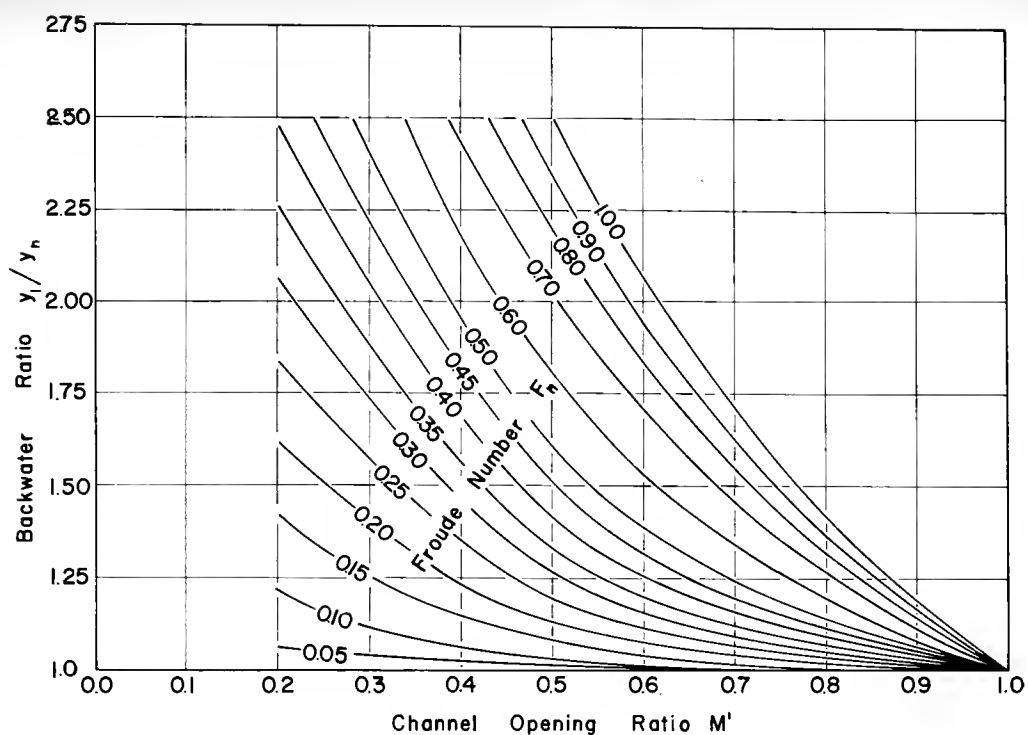


FIGURE 6a — BACKWATER RATIO VS CHANNEL OPENING RATIO  $L/b = 0$  SEMI-CIRC. SMOOTH CHANNEL

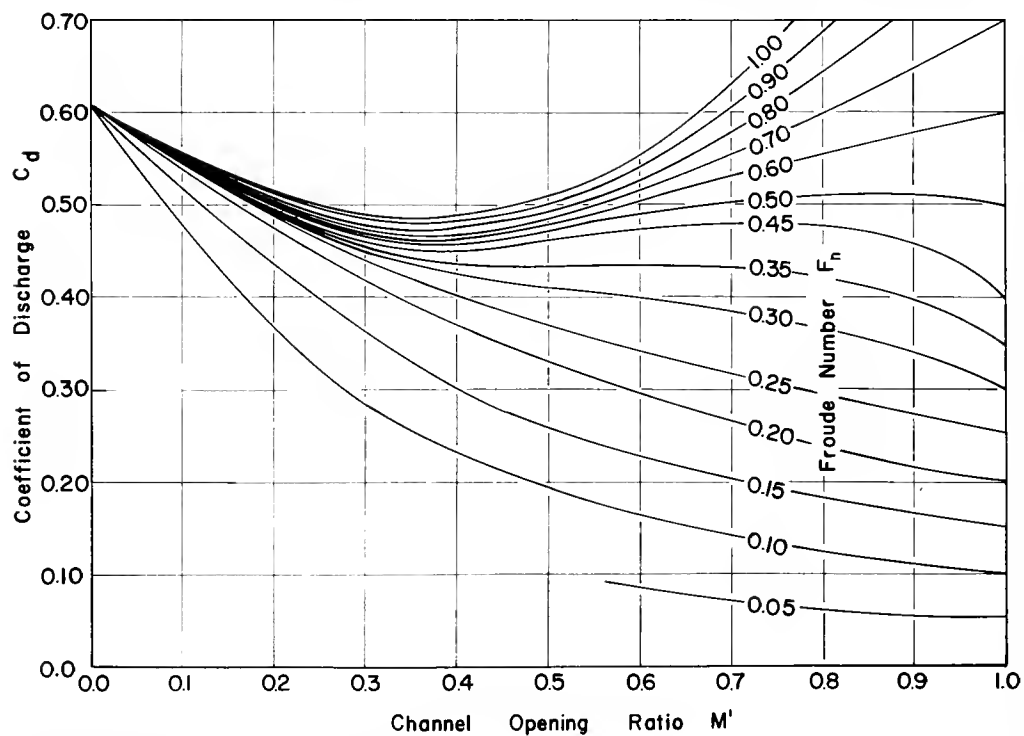
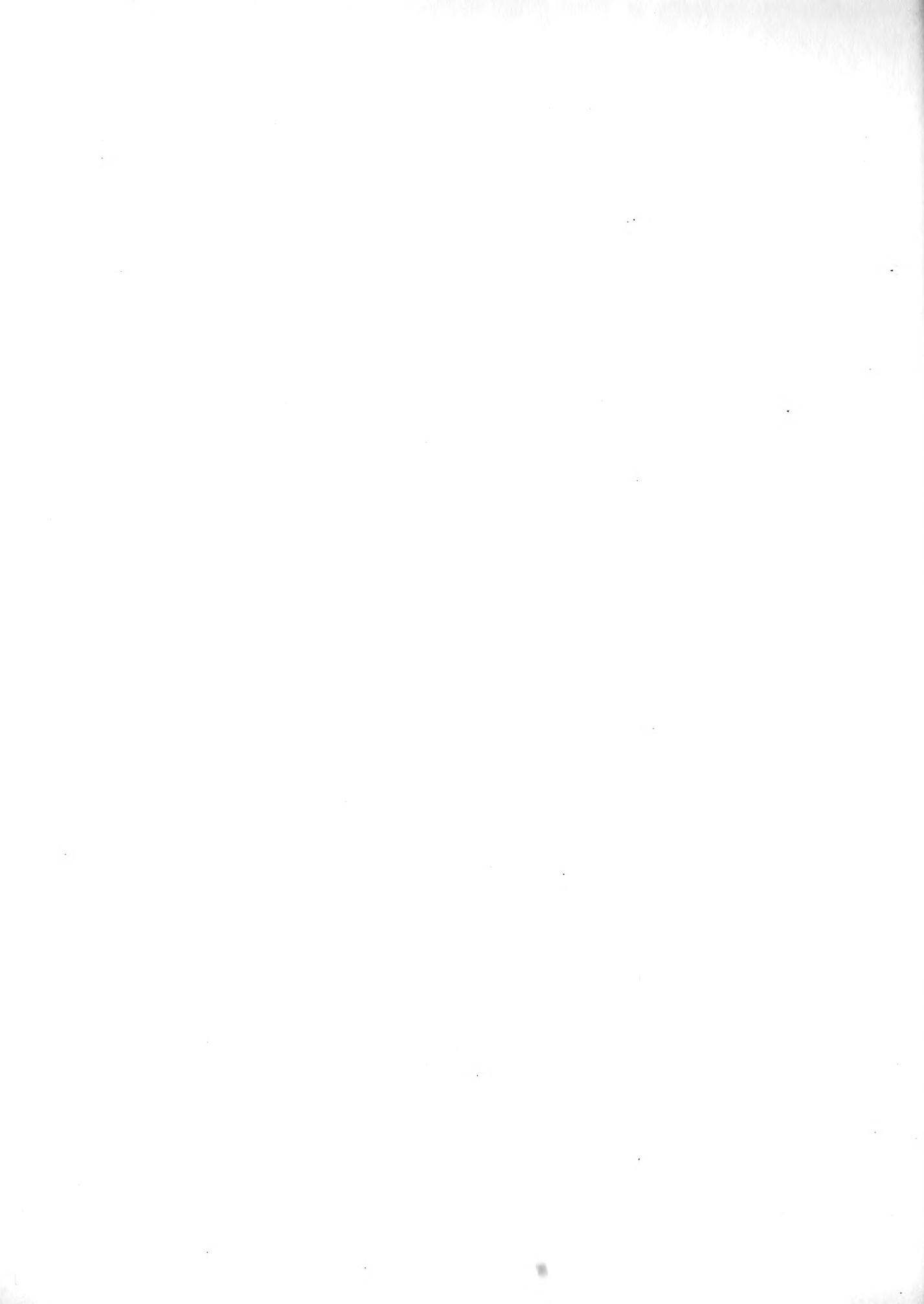


FIGURE 6b — DISCHARGE COEF. VS CHANNEL OPENING RATIO  $L/b = 0$  SEMI-CIRC. SMOOTH CHANNEL



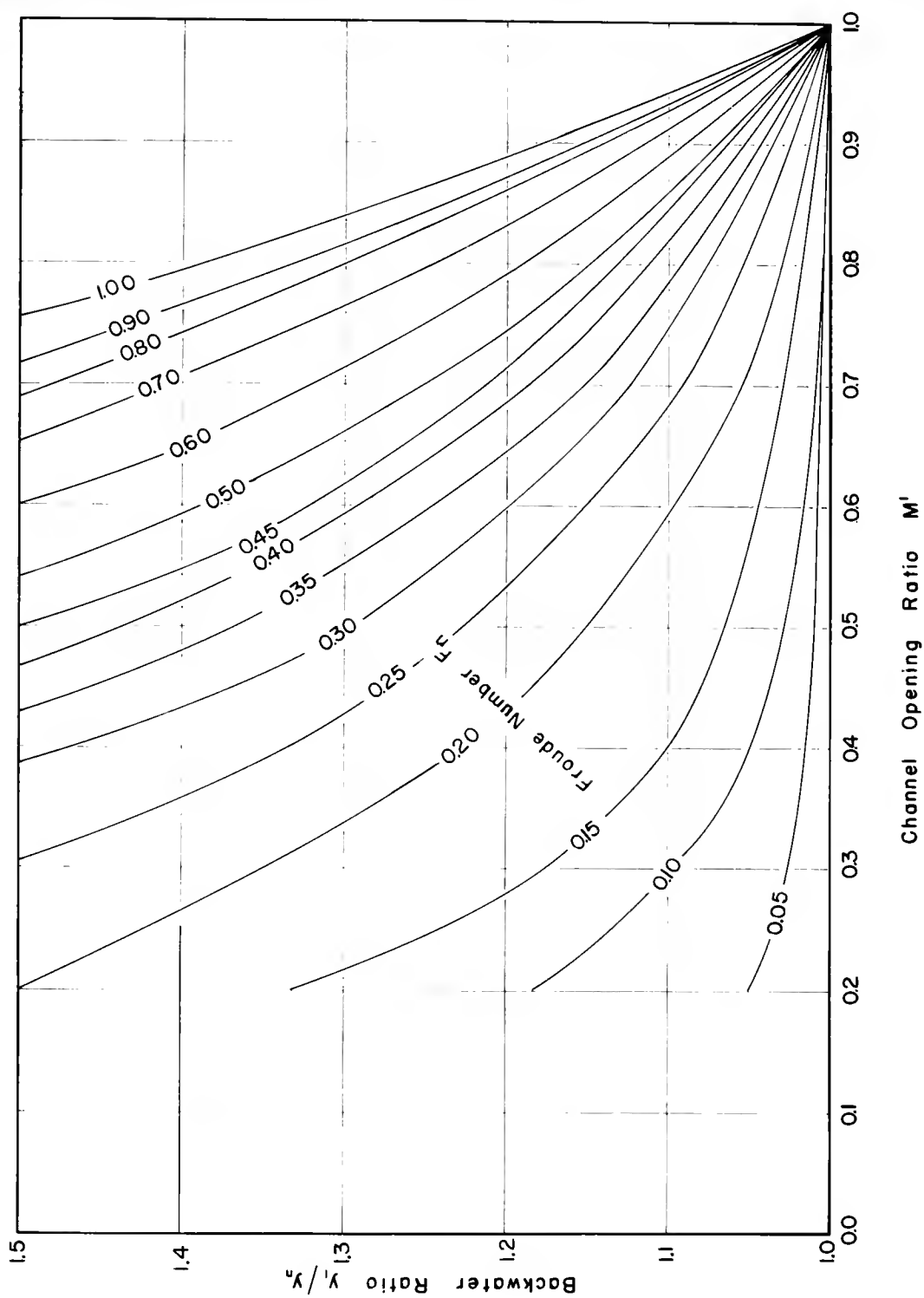


FIGURE 7a — BACKWATER RATIO VS CHANNEL  
OPENING RATIO  $L/B=0$  SEMI-CIRC.  
ROUGH CHANNEL  $y_1/y_n \leq 1.50$



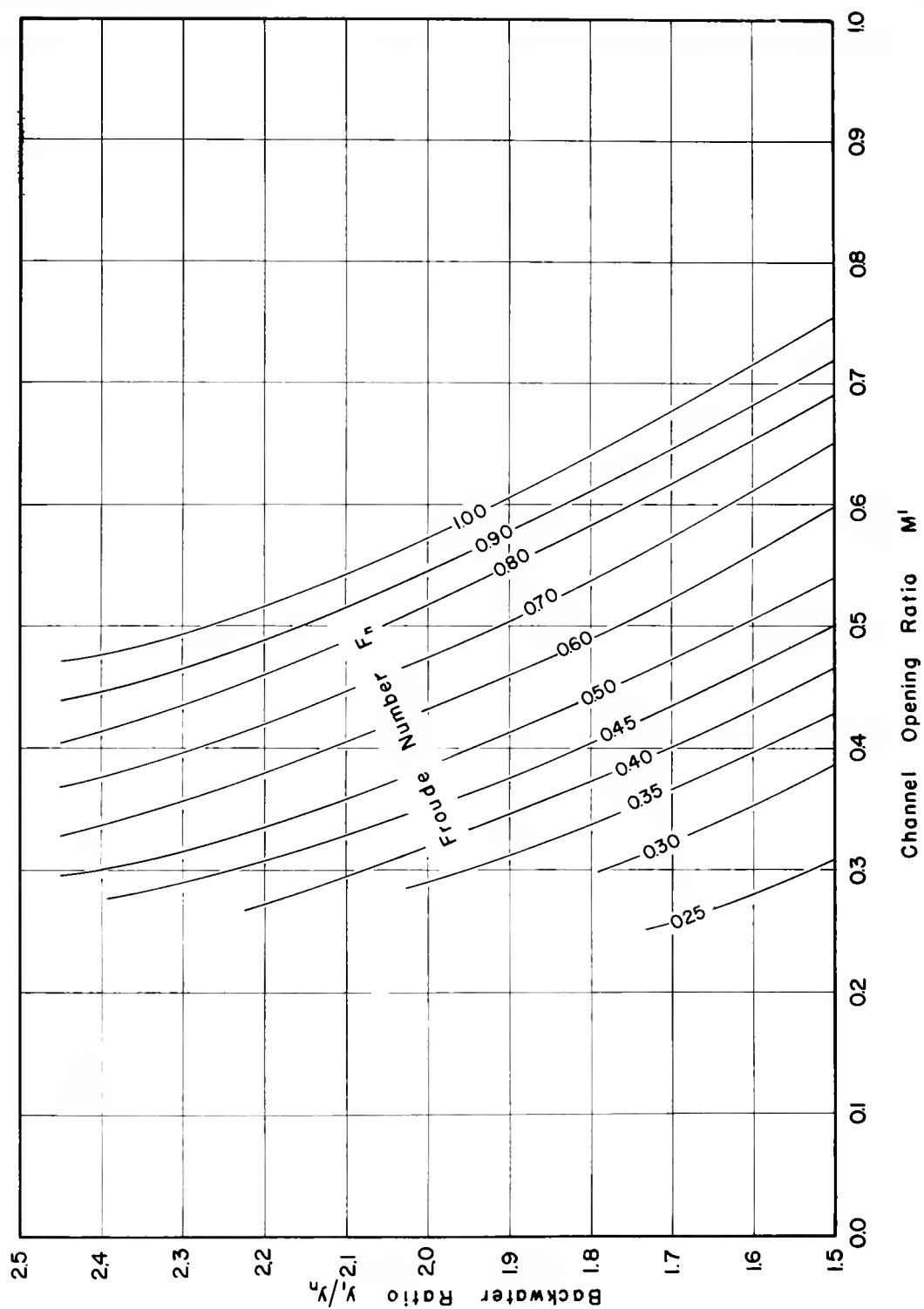


FIGURE 7b — BACKWATER RATIO VS CHANNEL  
OPENING RATIO  $L/b=0$  SEMI-CIRC.  
ROUGH CHANNEL  $1.50 \leq y_1/y_n \leq 2.50$



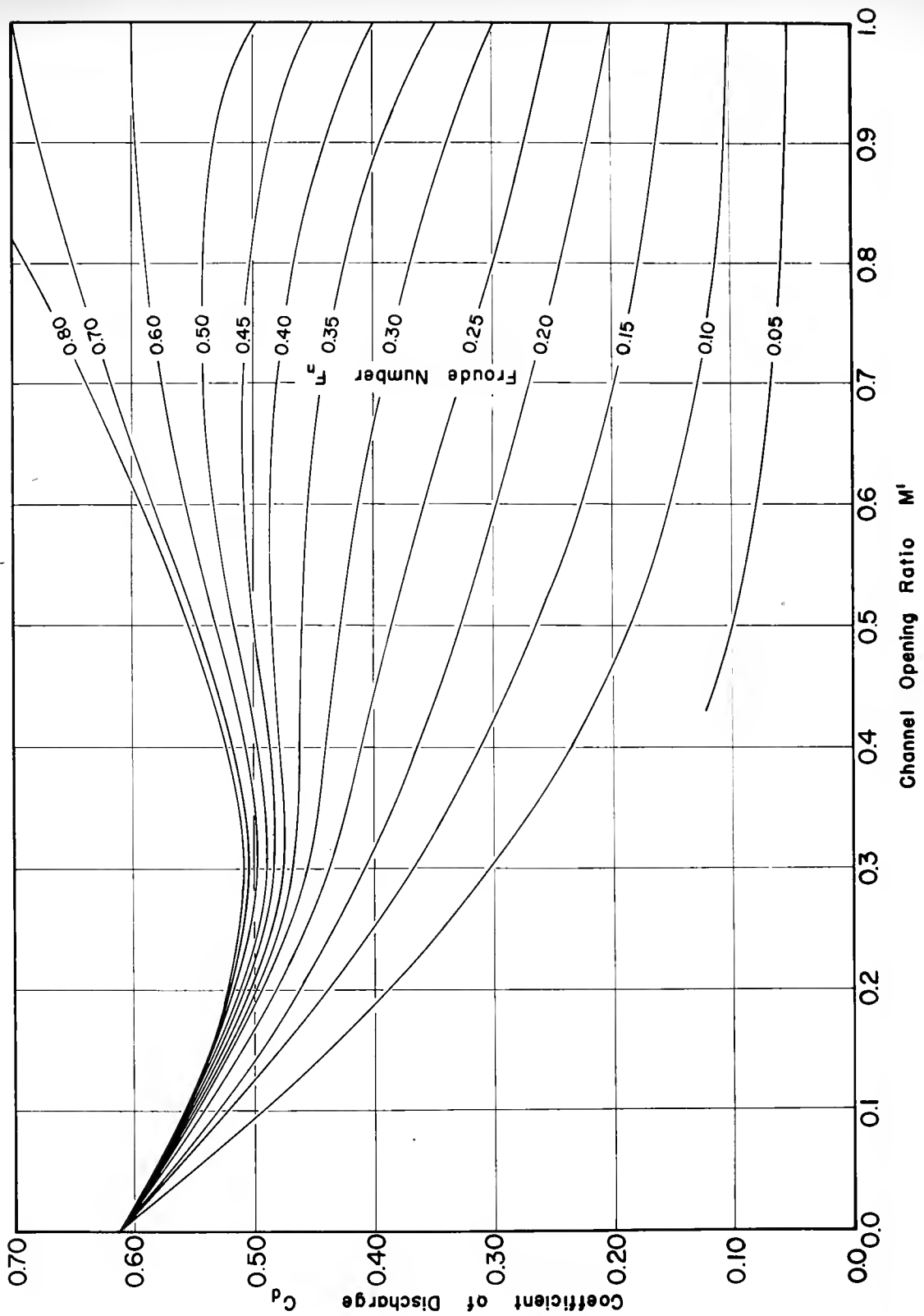


FIGURE 8 — DISCHARGE COEF. VS CHANNEL OPENING RATIO  $L/b=0$  SEMI-CIRC. ROUGH CHANNEL





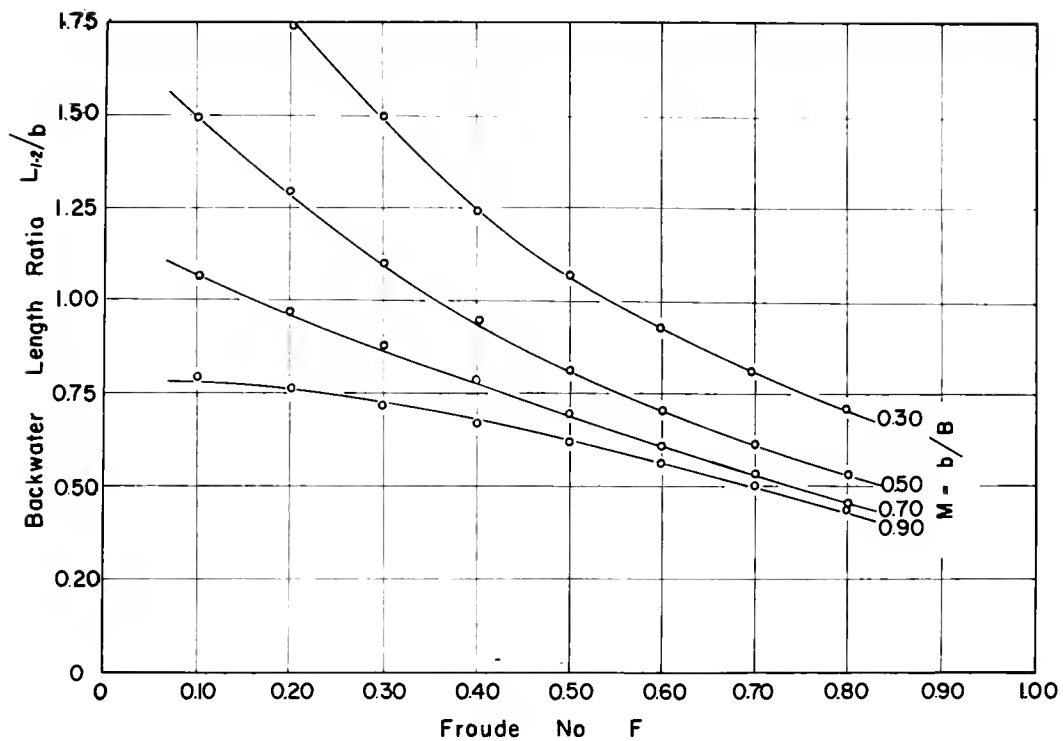


FIGURE 9a — LENGTH TO MAXIMUM BACKWATER

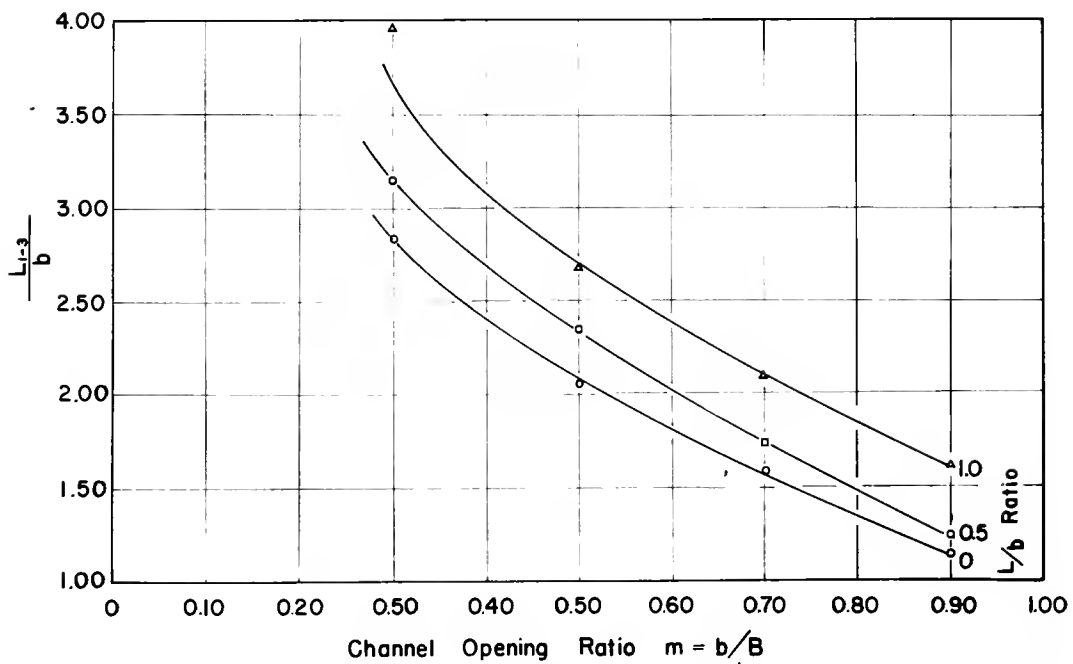


FIGURE 9b — LENGTH OF SURFACE PROFILE BETWEEN  $y_1$  &  $y_2$



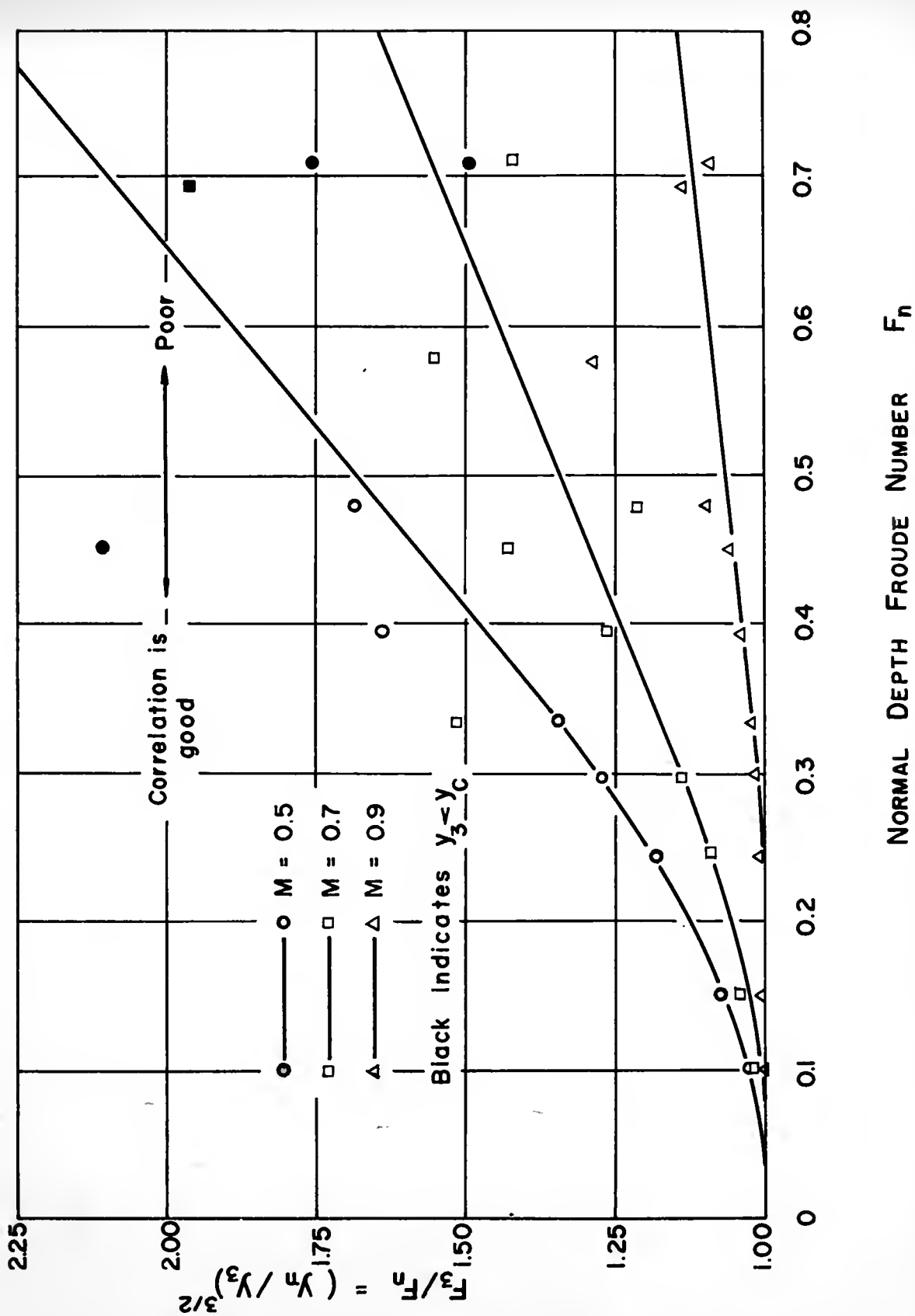


FIGURE 10 - CORRELATION CURVE OF  $F_3$



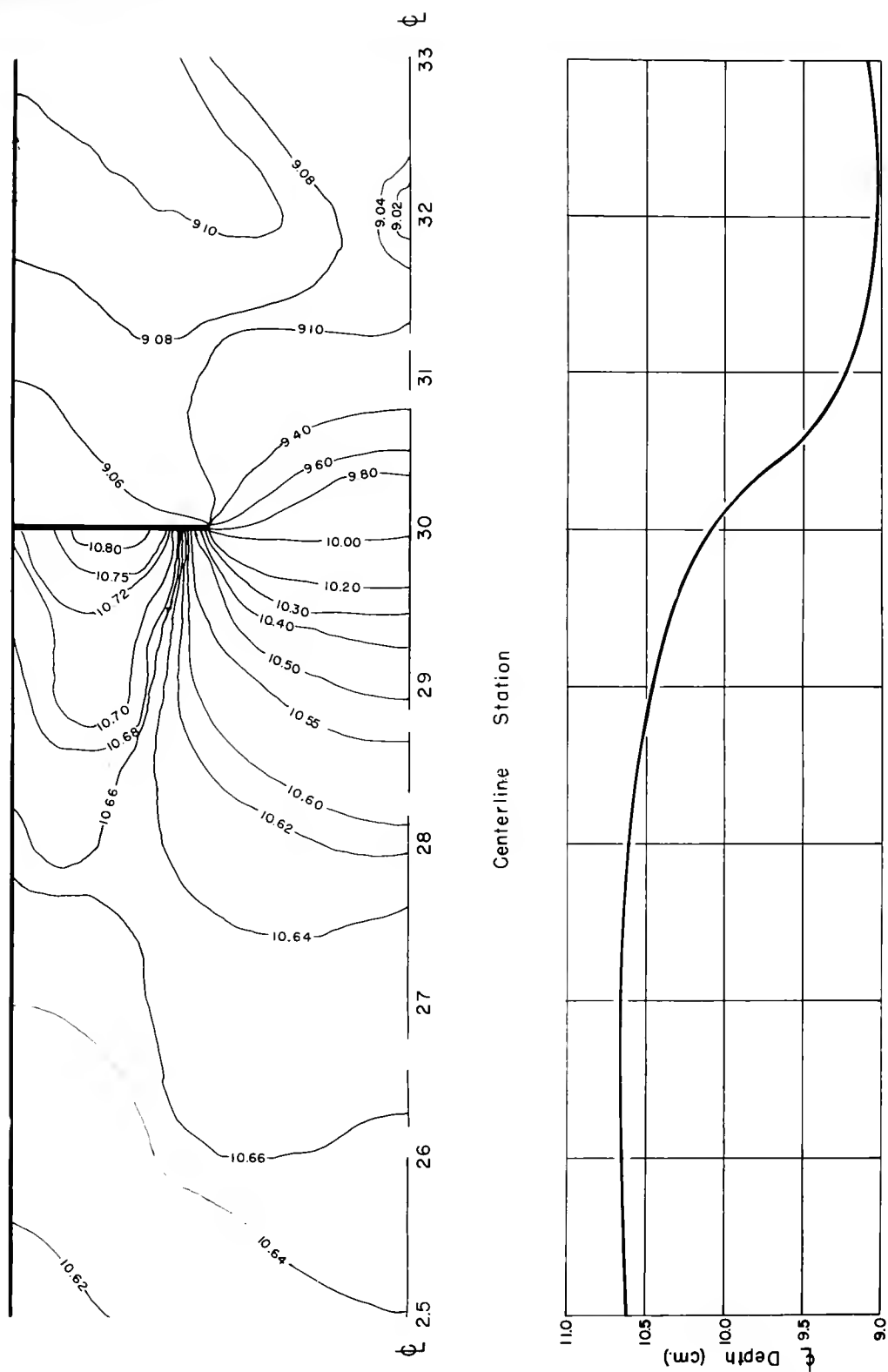
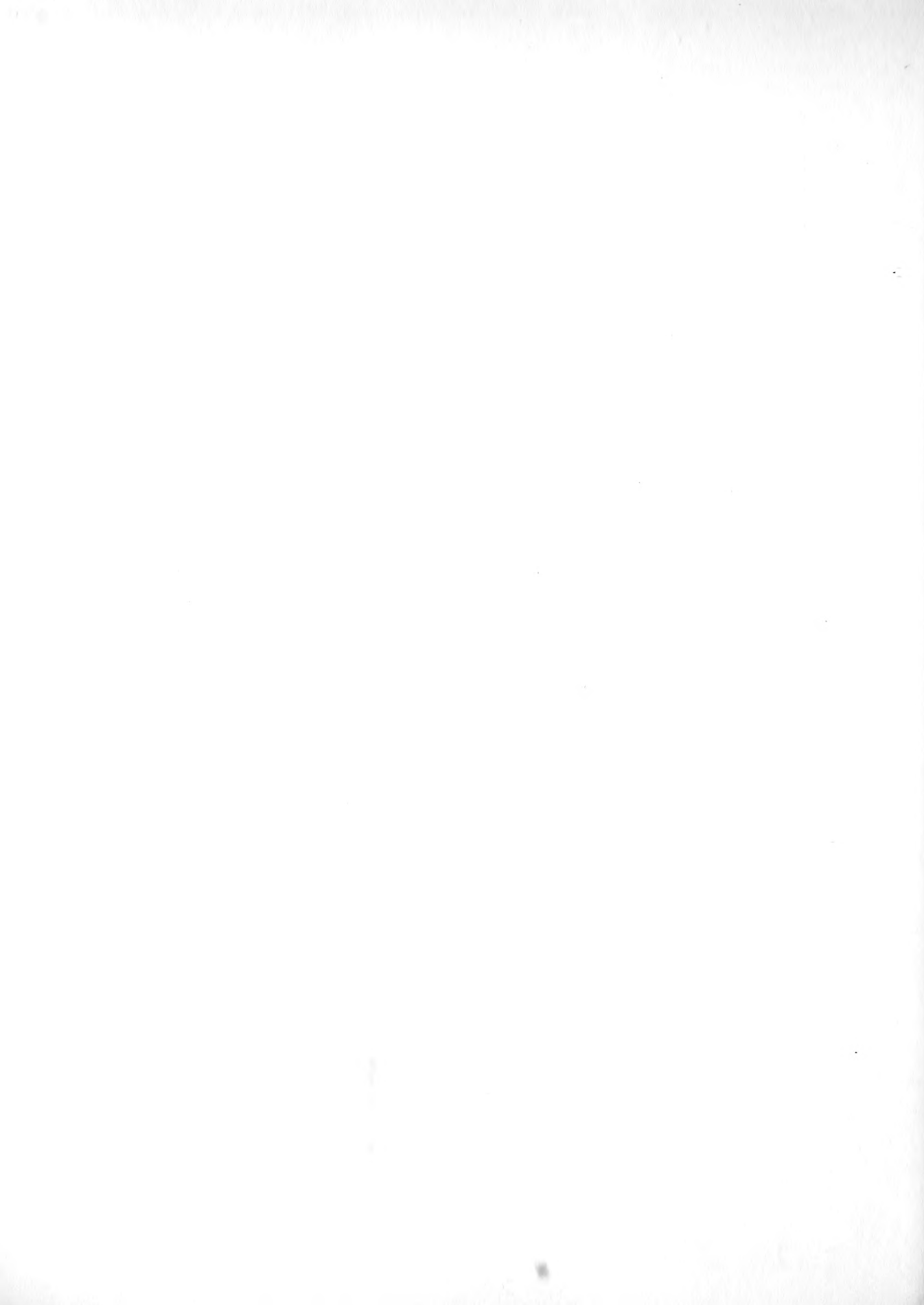


FIGURE II - SURFACE TOPOGRAPHY  $Q = 1$  CFS,  
 $S = 0.000584$ ,  $M = 0.5$ ,  $L/b = 0$



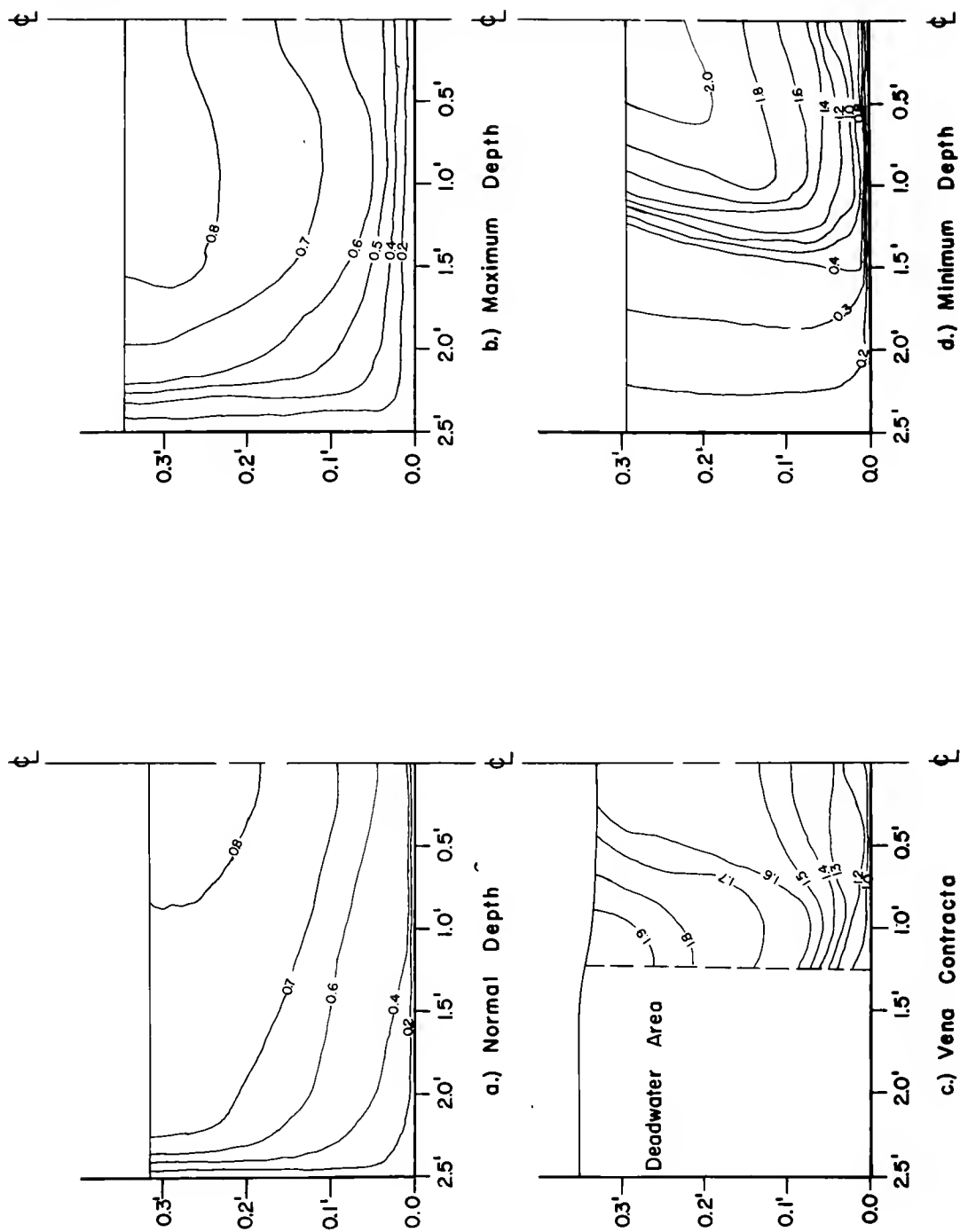


FIGURE 12 -ISOVEL DIAGRAMS IN FPS  $Q=10\text{CFS}$ ,  
 $S=0.000584$ ,  $M=0.5$ ,  $L/b=0$





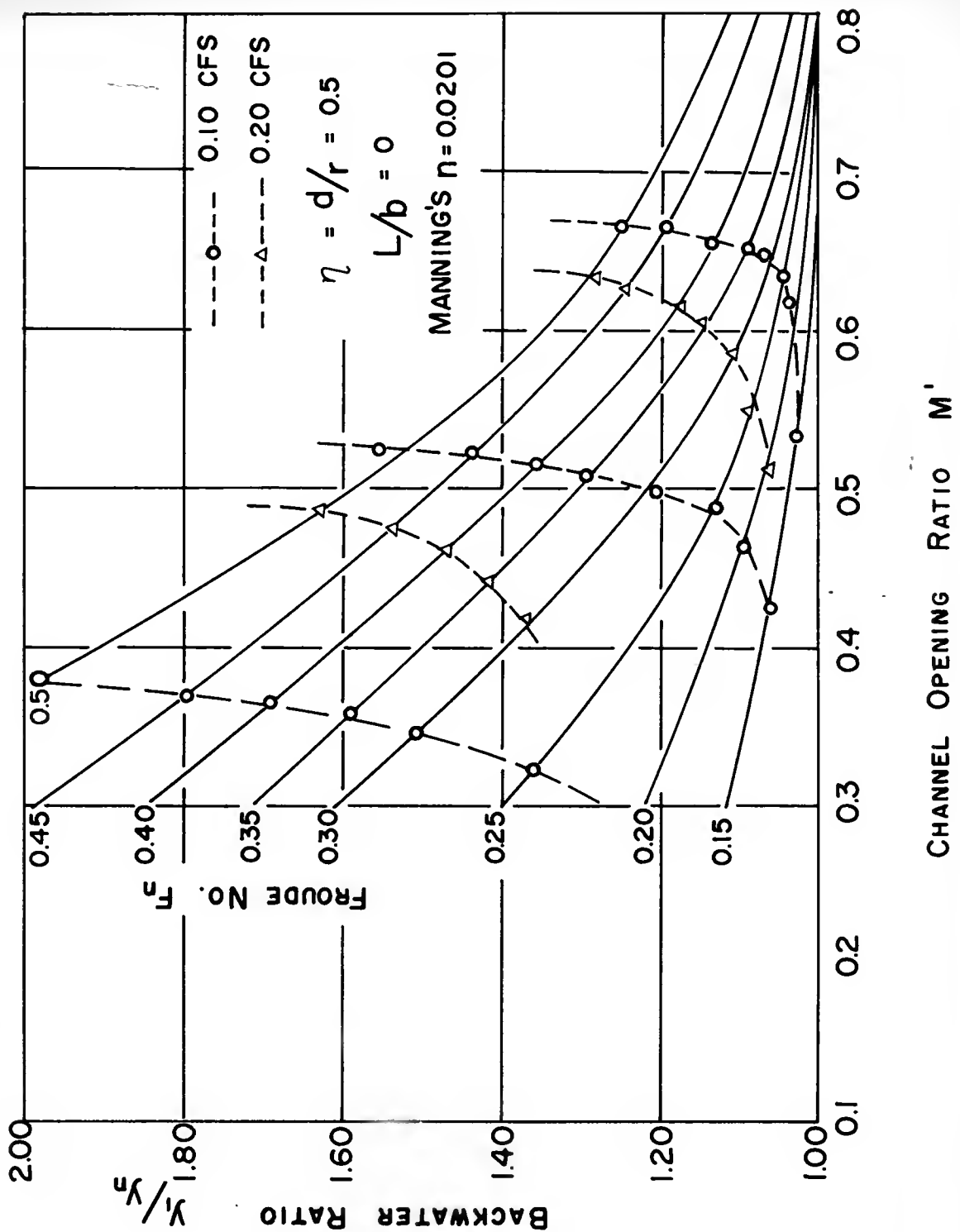


FIGURE 13- VARIATION OF THE BACKWATER RATIO FOR  
 SEGMENT ARCHES SMALL FLUME - ROUGH  
 BOUNDARIES



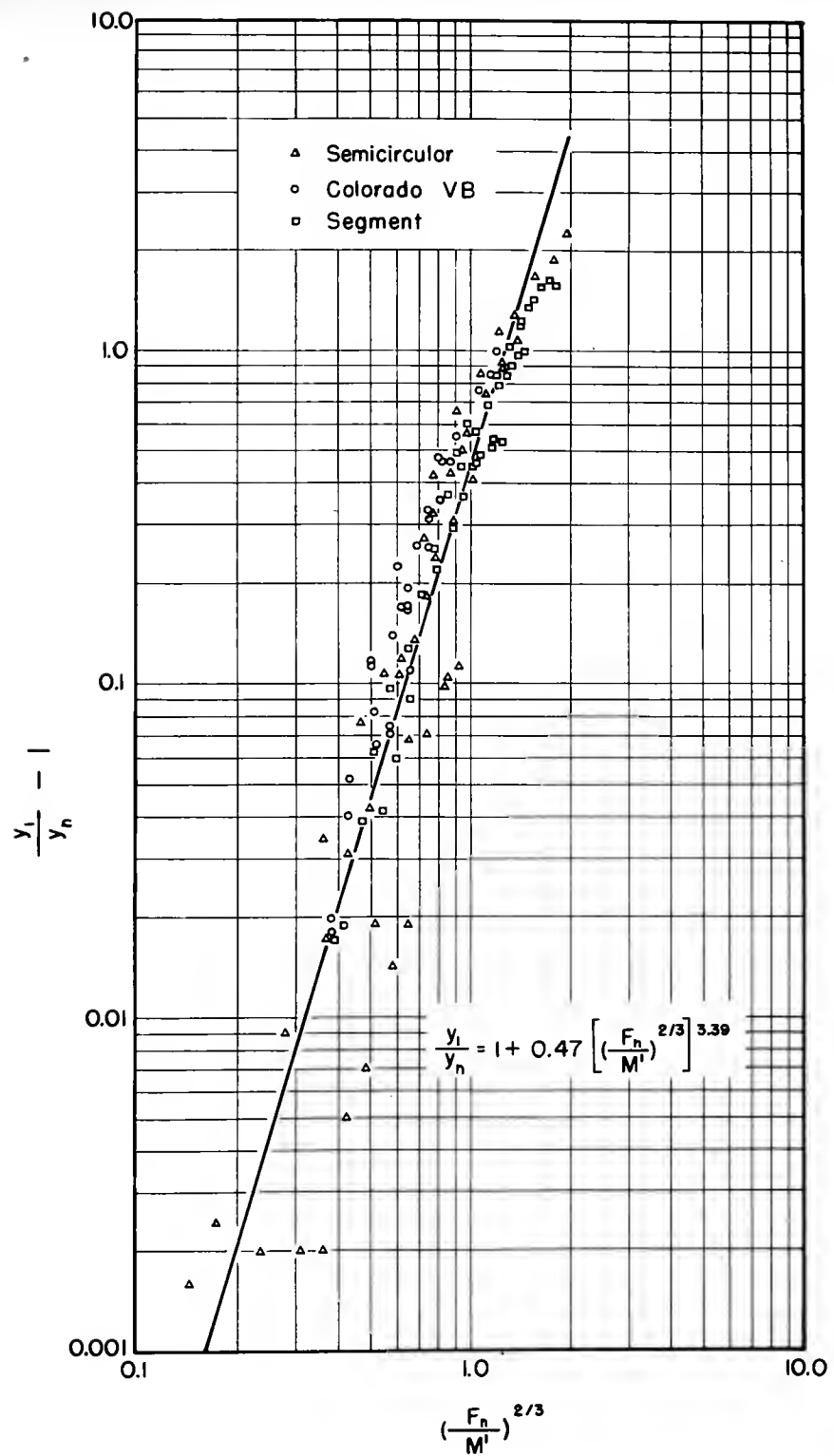


FIGURE 14 - GENERALIZED BACKWATER RATIO



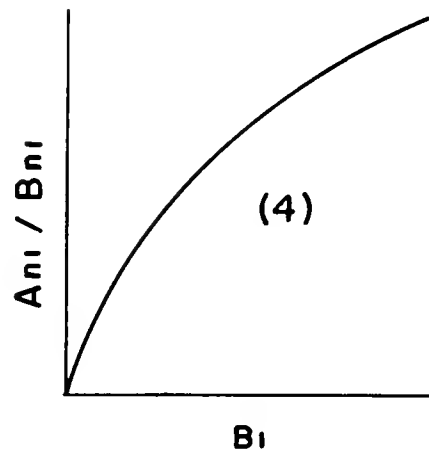
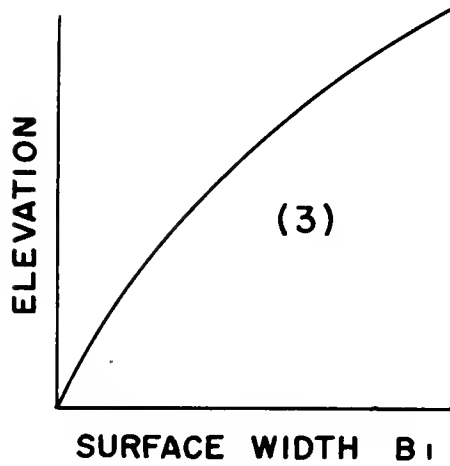
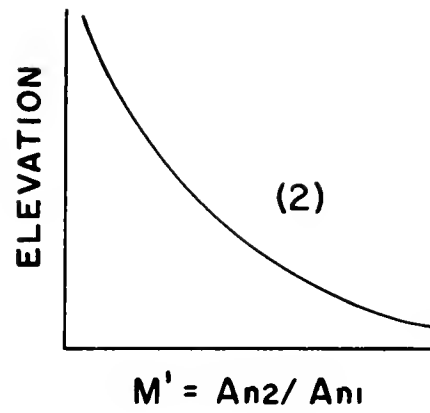
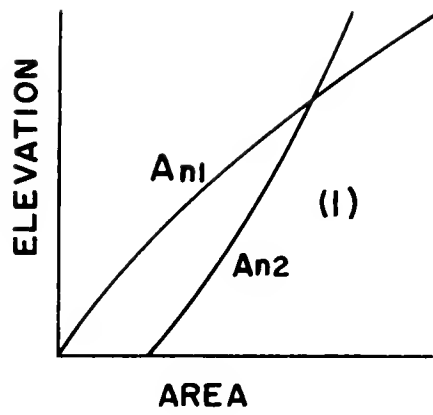


FIGURE 15 - WORKING CURVES FOR  
INDIRECT DISCHARGE MEASUREMENT

1000